

**Asia Pacific Research Initiative for Sustainable Energy  
Systems 2020 (APRISES20)**

**Office of Naval Research  
Grant Award Number N00014-21-1-2250**

**Ocean Thermal Energy Conversion (OTEC)  
Heat Exchanger Development  
(February to October 2024)**

**Task 6**

Prepared for  
Hawai'i Natural Energy Institute

Prepared by  
Makai Ocean Engineering

November 2024



**MAKAI OCEAN ENGINEERING**  
**ANNUAL REPORT**

SUBCONTRACT MA1991

Prepared For  
**HAWAII NATURAL ENERGY INSTITUTE**

1680 East West Road, POST 109  
Honolulu, HI, 96822  
USA

Prepared By  
**MAKAI OCEAN ENGINEERING**  
PO Box 1206, Kailua, Hawaii 96734

November 10, 2024

# TABLE OF CONTENTS

Table of Contents.....	i
List of Figures.....	iii
List of Tables.....	v
1. Introduction.....	6
2. TFHX Design Development.....	7
2.1. Cassette Design for Refrigerant Heat Exchangers.....	7
2.1.1. Condenser Design.....	7
2.1.2. Evaporator Design.....	9
2.2. Cassette Design for Commercial Seawater-Cooled Heat Exchanger (TFTX).....	10
2.3. Thin-Foil Air Conditioner (TFAC).....	13
2.4. Full-Length, Modular, Four-Port TFHX.....	13
2.5. Plate Spacing.....	15
2.5.1. Seawater Spacers.....	15
2.5.2. Plate Spacing.....	16
2.6. High Temperature High Pressure Development.....	19
3. TFHX Fabrication and Assembly.....	20
3.1. Plate Fabrication Improvements.....	20
3.2. Weld Defect Identification and Repair.....	20
3.3. Production Run Statistics.....	21
3.4. Future Areas of Focus.....	21
4. TFHX Performance Testing.....	23
4.1. 100-kW Test Station Operations.....	24
4.2. HX Facility Upgrades.....	24
4.3. Seawater-Ammonia Performance Testing.....	24
4.3.1. Seawater Pressure Drop.....	25
4.3.2. Ammonia Pressure Drop.....	26
4.3.3. Overall Heat Transfer Coefficient.....	27
4.3.4. Convective Coefficients.....	29
4.3.5. Heat Exchanger Approach Temperature.....	37
4.4. Discussion.....	42
5. Biofouling.....	44

5.1.	Intake Screen Testing .....	44
6.	Summary .....	45

## LIST OF FIGURES

Figure 2. Condenser Plate.....	7
Figure 3. Condenser installed on HX Tower.....	8
Figure 4. Evaporator plate .....	9
Figure 5. Evaporator installed in HX Tower .....	10
Figure 6. Modular approach. Modules can be arranged in series to meet the application’s cooling requirement. However, servicing requires disconnecting both hot and cold fluid flow paths. ....	11
Figure 7. Fixed-core approach. Only the outer cover needs to be removed for servicing. If more heat transfer area is needed, units can be placed in series or a single larger unit can be used. ....	12
Figure 8. TFAC installed in Makai’s Corrosion Lab.....	13
Figure 9. Seawater-seawater designs with (left to right) 1.7-mm, 1.5-mm, and 1.2-mm effective internal channel sizes.....	15
Figure 10. Seawater spacers could not support the weight of the stack during condenser assembly. Shims were used during evaporator assembly to aid in maintaining even plate spacing during assembly.....	15
Figure 11. (top, left to right). Plates were cut such that flow passed through the (top left) manifold insert + transition + 1” pattern, (top middle) manifold insert + transition zone, and (top right) manifold insert only. ....	17
Figure 12. The pressure drop vs flow rate was measured for each of the three configurations. Flow rate is the flow rate through each plate/manifold.....	17
Figure 13. Measured and predicted manifold pressure drop for different plate spacings. 2.12-mm is the current plate spacing. ....	18
Figure 14. For the same pressure drop, per plate flow rate can be doubled by increasing the internal channel size (from 0.9 mm in FL-3 to 1.70 mm in FL-16) and plate spacing (2.12-mm in FL-9 to 3.65-mm in FL-16, achieved by increasing insert thickness).....	18
Figure 20. Full-length TFHX module configured for counterflow condenser, evaporator, and seawater-seawater testing.....	23
Figure 21. Seawater pressure drop for all tested TFHX units.....	26
Figure 22. Ammonia pressure drop versus energy density for 12-plate TFHX units.....	27
Figure 23. U-value vs seawater velocity.....	28
Figure 24. U-value vs energy density.....	29
Figure 25. Seawater-side convective coefficients for TFHX units with pattern weld designs using the same dot weld (1.15mm weld diameter) but different weld spacings and expansion pressures. External channel size is shown after the unit number.....	30

Figure 26. Seawater-side convective coefficients for TFHX units with the same pattern weld design (3.11mm circle weld diameters at 9.5mm spacing) but different expansion pressures. External (seawater) channel size is shown after the unit number. ....31

Figure 27. Evaporator seawater convective coefficients. TFHX units are listed from smallest seawater channel (TFHX-FL2) to largest (TFHX-FL8).....33

Figure 28. Condenser seawater convective coefficients. TFHX units are listed from smallest seawater channel (TFHX-FL2) to largest (TFHX-FL6).....35

Figure 29. Ammonia-side convective coefficients for evaporator and condenser. TFHXs are listed from smallest ammonia effective channel (TFHX-FL8/-FL1) to largest (TFHX-FL3)...36

Figure 30. Evaporator approach temperature vs pumping power at different energy densities. ...39

Figure 31. Condenser approach temperature vs pumping power at different energy densities.....41

Figure 32. Comparison of evaporator designs in OTEC system. ....42

Figure 33. Comparison of condenser designs in OTEC system. ....43

Figure 39. Strainer inspection revealed accumulated shells at the bottom and fibrous mats on the sides. ....44

## LIST OF TABLES

Table 1. Overview of full-length configurations constructed to date. ....	14
Table 2. Production Statistics .....	21
Table 3. Overview of TFHX test units.....	23

## 1. INTRODUCTION

Makai Ocean Engineering has been developing Thin Foil Heat Exchangers (TFHX) for use in seawater-refrigerant, air-water, and water-water applications. This report summarizes work performed between February 2024 – October 2024.

In this period, Makai’s efforts included improving TFHX fabrication and assembly methods, characterization of TFHX thermal performance, and investigation of biofouling mitigation methods.

### *TFHX Design Development*

Makai demonstrated the fabrication and assembly of two cassette-style, seawater-ammonia, 2-MW<sub>thermal</sub> TFHXs (one evaporator and one condenser).

Makai has also been working on designs for large-scale, seawater cooling applications that incorporate an in-situ cleaning system and accessibility to the heat exchanger core. The in-situ cleaning system extends the manual servicing period and the accessible design minimizes maintenance down time when servicing is eventually required.

Finally, Makai has been exploring options to increase the internal fluid flow rates to make the TFHX more competitive in applications that already use plate-and-frame heat exchangers.

### *TFHX Fabrication and Assembly*

Makai continued to improve the fabrication fixtures, parameters, procedures, and quality control capabilities to reduce the fabrication time while improving plate success rates. Makai also tested the existing assembly fixtures and procedures and worked on improvements for the next iteration.

### *TFHX Performance Testing*

Makai tested one TFHX in the seawater-ammonia configuration and fabricated and tested two TFHXs in the seawater-seawater configuration.

### *Biofouling*

Makai continued ongoing in-situ cleaning and baseline tests and developed additional prototypes. A new submerged test was also started in this period.

## 2. TFHX DESIGN DEVELOPMENT

In this period, Makai's TFHX design efforts focused on cost-effective designs for large seawater-cooled heat exchangers (including seawater spacer improvements) and new 4-port pattern designs.

### 2.1. CASSETTE DESIGN FOR REFRIGERANT HEAT EXCHANGERS

Makai previously reported on a new cassette-style design for large-scale heat exchangers. In this period, Makai (under separate funding) built two cassette-style seawater-ammonia TFHXs at the 2-MW<sub>thermal</sub> scale. Both heat exchangers are installed on the new OTEC Heat Exchanger Test Facility and performance testing will take place in the next period.

#### 2.1.1. Condenser Design

The condenser has 145.9 m<sup>2</sup> of heat transfer area. The same manifold inserts as the full-length, 4-port plate are used, producing a plate spacing of 2.12 mm. The plate design is based on FL-4 with an internal channel size of 0.68 mm and an external channel size of 1.19 mm (Figure 1).

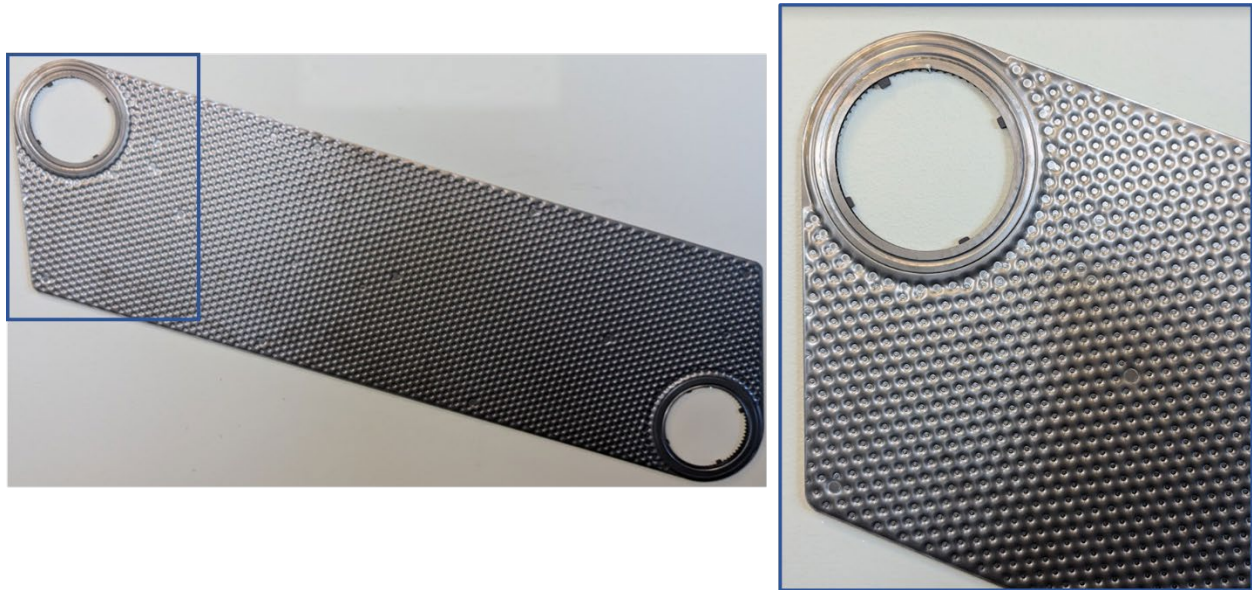


*Figure 1. Condenser Plate*

The condenser plates are installed in two stacks (one above the other) at a 15° angle to promote ammonia liquid drainage. Ammonia and seawater flow is split (in parallel) between the two stacks (Figure 2). Ammonia vapor enters through the top manifold and exits as liquid through the bottom manifold. The seawater flow direction is opposite of the ammonia flow direction; cold seawater enters closest to the ammonia exit manifold and exits closest to the ammonia inlet manifold. This counterflow orientation is the same as the previously tested FL-4 configuration. Some cross flow may occur as ammonia starts to condense and liquid drips vertically down the plate instead of strictly horizontally towards the exit manifold. Makai expects the condenser performance to match FL-4. Figure 2 also shows Makai's condenser (which has the same 2-MW capacity) in the same frame as the APV condenser; the TFHX is substantially smaller volume and weighs less.

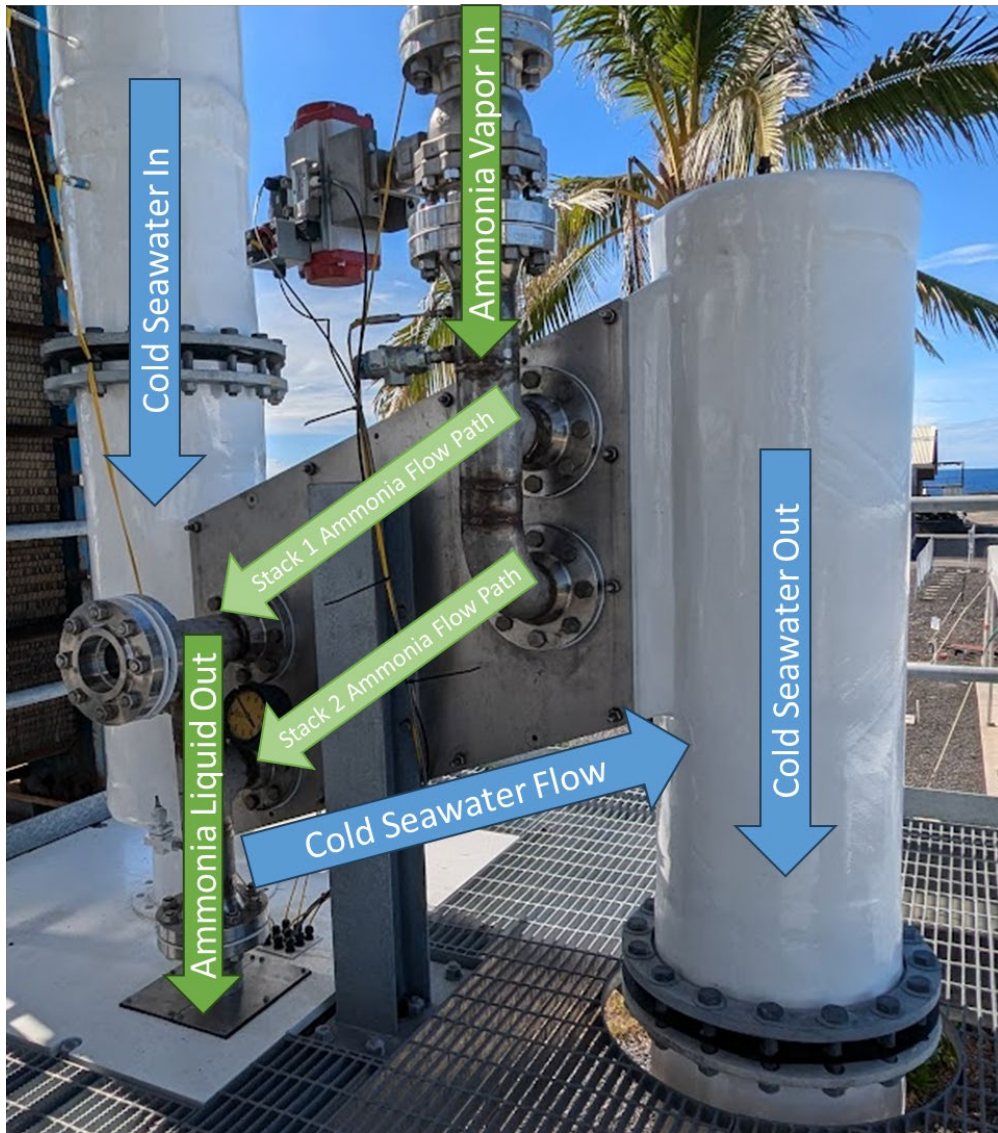
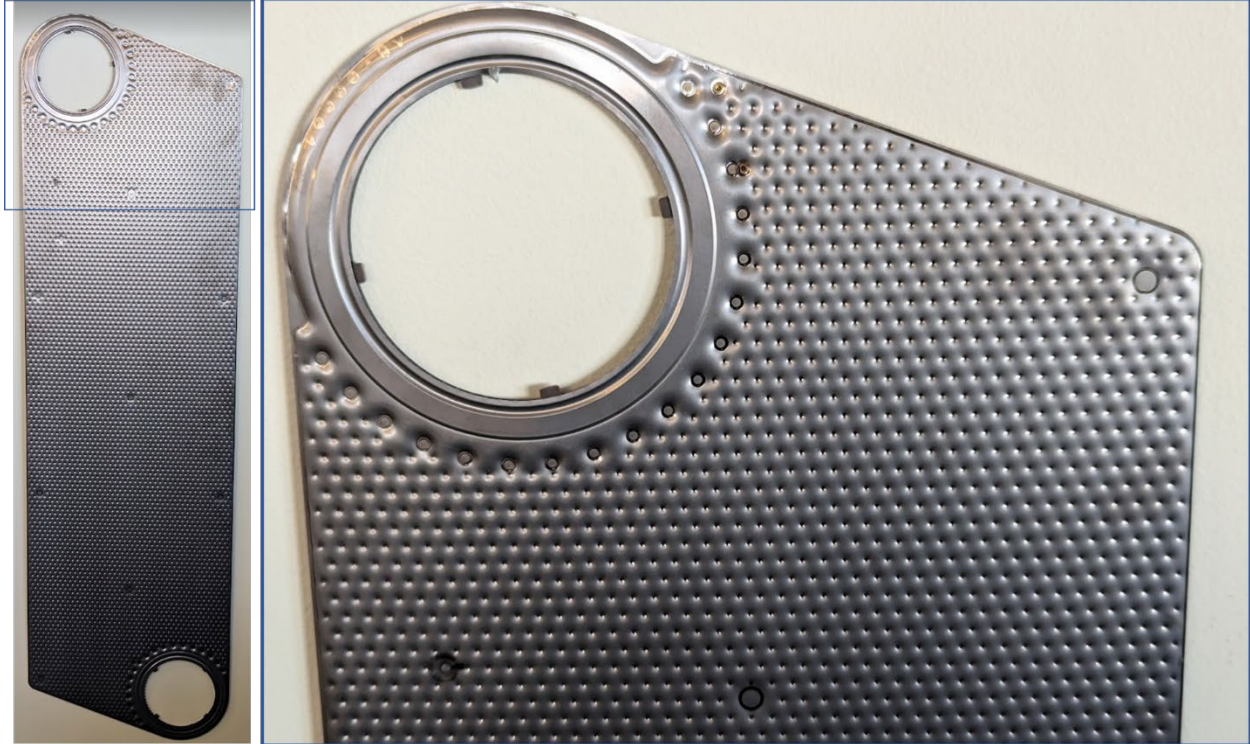


Figure 2. Condenser installed on HX Tower

### 2.1.2. Evaporator Design

The evaporator has 300 plates, arranged in two stacks of 150 plates each, for a total 144 m<sup>2</sup> of heat transfer area at 2.12-mm plate spacing. The plate design is based on FL-12 with internal and external channel sizes of 0.52 mm and 1.35 mm, respectively (Figure 3).



*Figure 3. Evaporator plate*

The evaporator is arranged in a vertical, cross-flow configuration. The two plate stacks are side by side such that the ammonia flow is split (in parallel) between the two stacks but the seawater flow is in series. For initial testing, the ammonia flow will be in a falling film orientation where ammonia liquid enters from the top manifold and vapor exits from the bottom manifold (Figure 4). The falling film configuration is expected to improve evaporator performance because it should eliminate a standing section of ammonia liquid (and the associated loss of effective heat transfer area). With the seawater flow in series, the second stack (in the seawater flow direction) is expected to have lower duty than the first stack *if* the ammonia flow rates were the same in both stack due to the colder warm seawater temperature entering the second stack. Makai expects ammonia flow distribution can be tuned to maximize the total evaporator duty.



*Figure 4. Evaporator installed in HX Tower*

## 2.2. CASSETTE DESIGN FOR COMMERCIAL SEAWATER-COOLED HEAT EXCHANGER (TFTX)

Makai has been focused on developing TFHX designs that meet a current market need to provide a clear path to commercialization. Seawater-cooled applications take advantage of the TFHX's titanium, corrosion resistant construction and our biofouling control system. All the applications Makai has evaluated require external fluid containment rather than a pass-through design that was used at Cyanotech or for the TFAC. Most commercial applications that use seawater for cooling use plate-frame heat exchangers where water is the hot fluid; Makai is still searching for commercial contacts that use refrigerants as the hot fluid.

For the seawater-cooling market, Makai is developing concepts that are serviceable (automated with a manual backup) and cost-competitive. To meet the serviceability requirement, Makai has been developing cross-flow concepts using the cassette design. Cost-effective requirements will drive the design towards larger heat exchangers so the housing costs are a smaller proportion of the overall cost.

Makai's previous TFPX prototype was intended to address the seawater-cooled market but in the scaled-up design, serviceability or handling of the full-size plate stack would be challenging. A full-scale TFPX was intended to fit ~100 1-m long plates in an 18" pipe. Accessing the plate stack would require disconnecting the pipe section and clearance to slide the 1-m long stack out. Re-assembly would require sliding the stack back in and re-aligning the internal fluid manifold seals.

These steps are likely more difficult at the full-scale than at the prototype scale. Furthermore, the fluid flow paths are arranged in a counterflow configuration in the TFPX. With our recent progress in biofouling mitigation, Incorporating an automated biofouling cleaning mechanism is challenging in counterflow; current prototype designs are for the cross-flow configuration.

Makai is evaluating two design approaches that have integrate in-situ cleaning capability. One approach is modular and requires interrupting both internal and external flow paths for servicing (Figure 5). The other approach keeps the internal fluid flow path intact and the heat exchanger core in place for servicing (Figure 6).

The modular approach can be tailored to an application by adding modules in series to meet the heat transfer area requirements. However, because both fluid flow paths are broken for servicing, more sealing surfaces have to be re-aligned prior to returning the unit to service. This can be more challenging compared to the fixed core approach, but likely still more advantageous compared to servicing plate-and-frame heat exchangers where each individual plate must be re-sealed prior to operation.

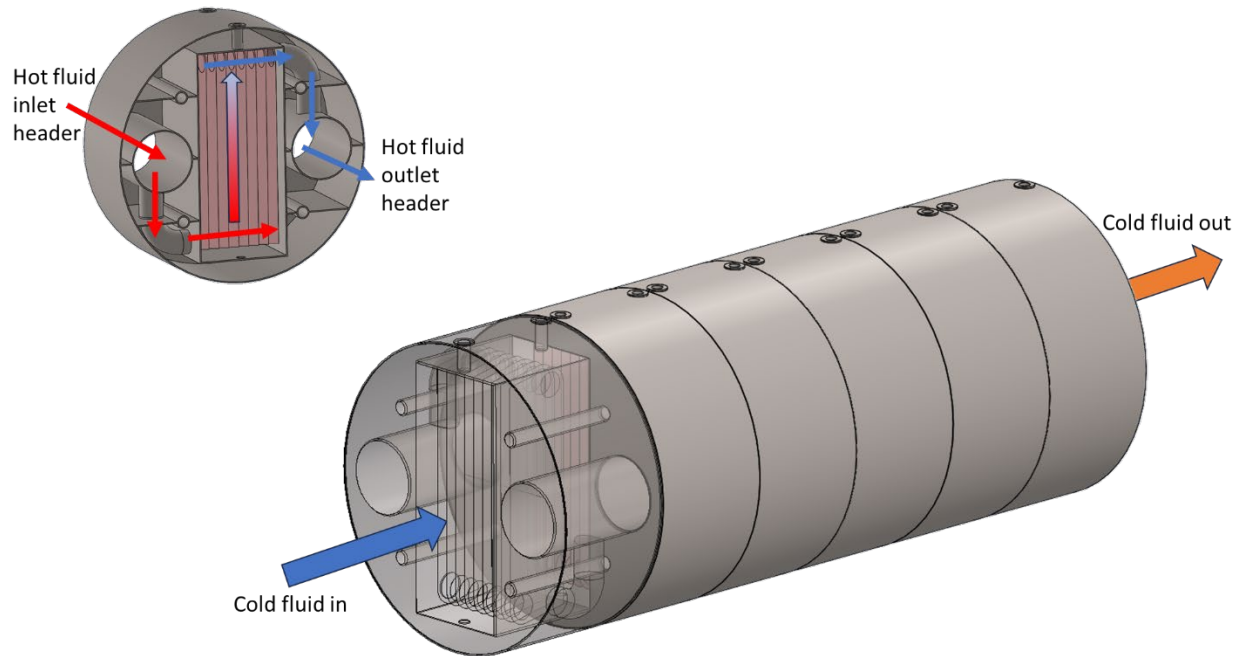


*Figure 5. Modular approach. Modules can be arranged in series to meet the application's cooling requirement. However, servicing requires disconnecting both hot and cold fluid flow paths.*

In the fixed core approach, the amount of heat transfer area per unit is fixed and a cover or access panel is removed to inspect or perform maintenance. Only one or two interfaces that have to be re-sealed to return the unit to operation. If more heat transfer area is needed, either a larger model or multiple units can be used in parallel (or in series).

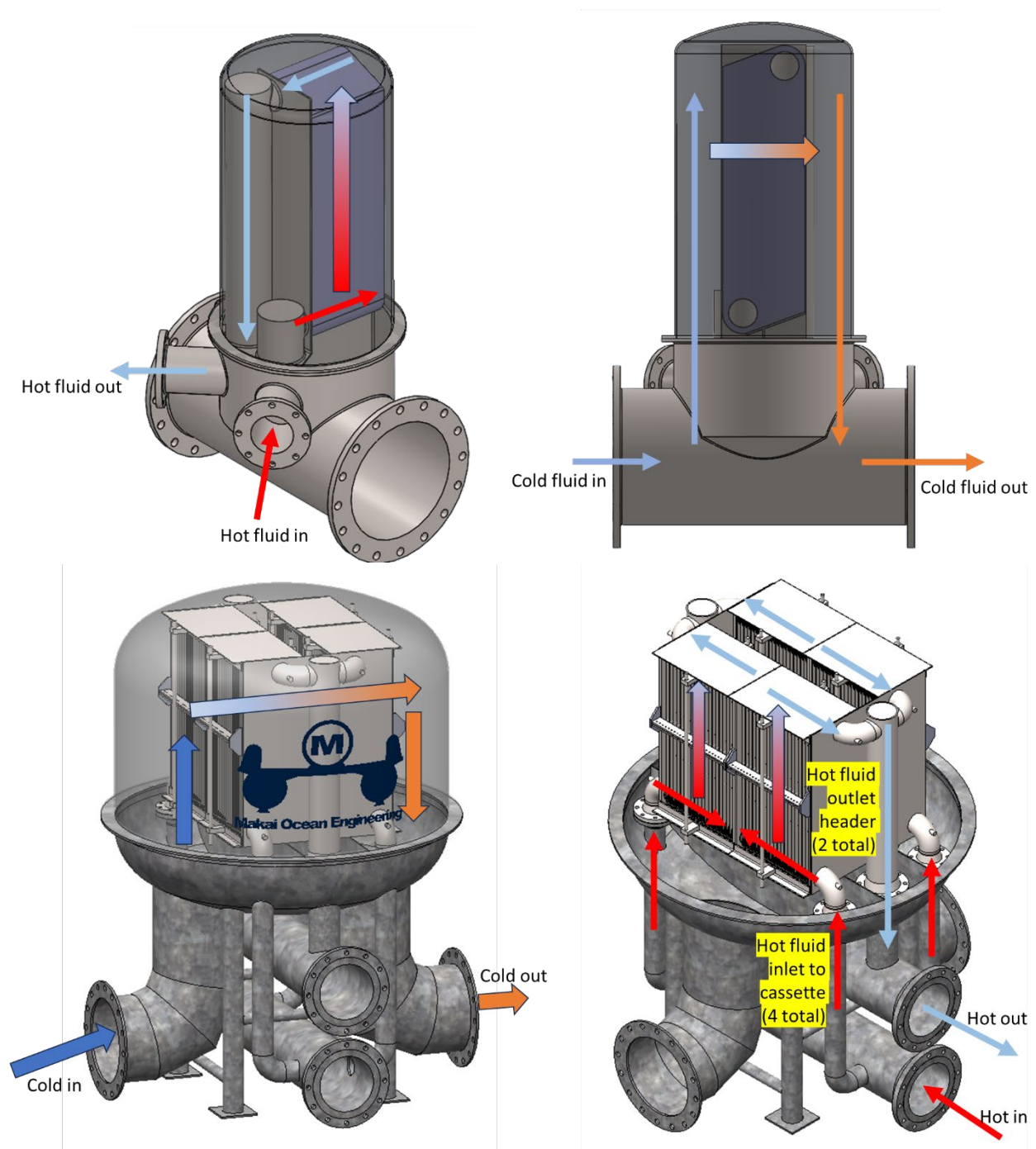


*Figure 6. Fixed-core approach. Only the outer cover needs to be removed for servicing. If more heat transfer area is needed, units can be placed in series or a single larger unit can be used.*

Makai is still evaluating the two approaches and refining concepts within each approach before settling on a design. Housing components can be expensive, driving designs towards larger heat exchangers to maintain a higher ratio of heat exchanger core cost compared to housing cost.

However, larger heat exchangers have higher associated flow rates (both internal and external) and Makai is working on solutions to lower the internal fluid pressure drop at high water flow rates (discussed in more detail in Section 2.5.2).

### 2.3. THIN-FOIL AIR CONDITIONER (TFAC)

Blue Ocean Mariculture (BOM) expressed interest in Makai's Thin-Foil Air Conditioning (TFAC) unit which uses an off-the-shelf box fan and cold seawater to provide cooling and dehumidification for environmental control (Figure 7). Although Makai delivered a TFAC unit to BOM, it was never installed. Makai installed the TFAC in our own corrosion lab after the existing AC fan unit failed. The TFAC is a simple pass-through design, where cold seawater passes through the internal channel of the plates, while air flows through the stack. Twenty-four mid-length plates were used in these units (two units were constructed), with a total of 4.8m<sup>2</sup> heat exchanger area.

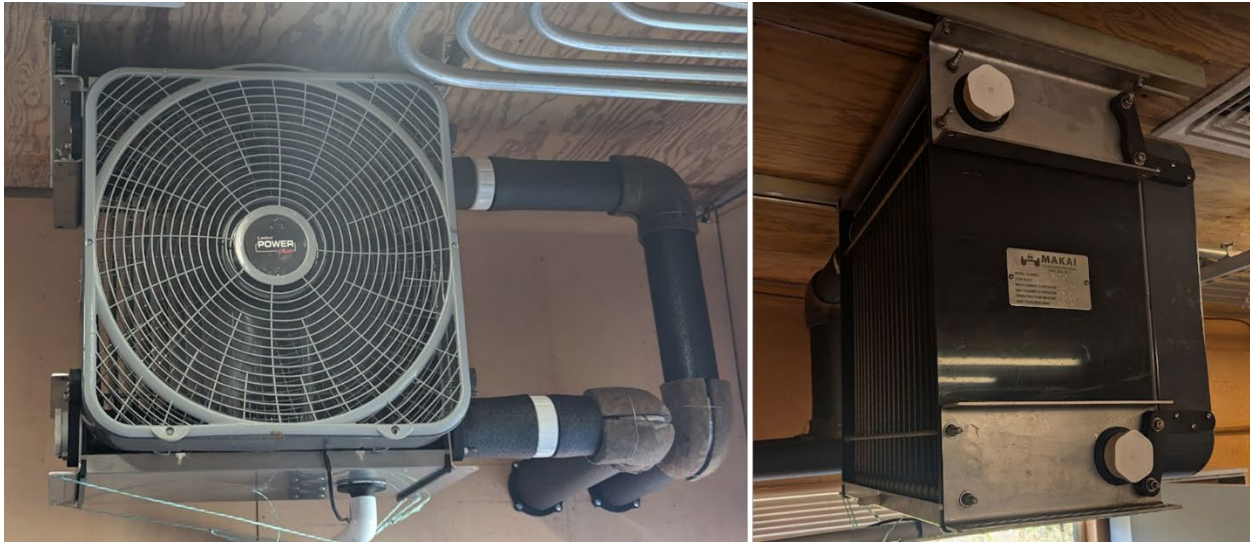


*Figure 7. TFAC installed in Makai's Corrosion Lab.*

### 2.4. FULL-LENGTH, MODULAR, FOUR-PORT TFHX

Makai developed three new pattern designs for seawater-seawater applications (Figure 8 and Table 1) and fabricated two heat exchangers in the four-port modular configuration. Two of the new designs were performance tested in the 100-kW Test Station in this period and two more performance tests are planned for the next period. Performance testing results are discussed separately in Section 4.

*Table 1. Overview of full-length configurations constructed to date.*

		# Plates	Plate Spacing [mm]	Foil Thickness ["]	Internal Channel Size [mm]	External Channel Size [mm]	HX Area [m2]	# Welds	Burst Pressure [psi]	Expansion Pressure [psi]
<b>Seawater-ammonia</b>	<b>TFHX-FL1</b>	24	2.12	0.005	0.589	1.275	10.32	9777	600	478
	<b>TFHX-FL2</b>	24	2.12	0.005	0.9	0.964	10.32	2730	563	500
	<b>TFHX-FL3</b>	12	4.24	0.005	0.9	0.964	5.16	2730	563	500
	<b>TFHX-FL4</b>	24	2.12	0.005	0.78	1.084	10.32	2730	563	414
	<b>TFHX-FL5</b>	12	2.12	0.005	0.78	1.084	5.16	2730	563	414
	<b>TFHX-FL6</b>	6	4.24	0.005	0.78	3.202	2.58	2730	563	414
	<b>TFHX-FL7</b>	12	2.12	0.005	0.503*	1.362*	5.16	4088	438	350
	<b>TFHX-FL8</b>	6	4.24	0.005	0.562	3.421	2.58	9554	725	643
	<b>TFHX-FL9</b>	12	2.12	0.005	0.560*	1.304*	5.16	6853	585	500
	<b>TFHX-FL10</b>	12	2.12	0.005	0.838	1.026	5.16	3738	286	245
	<b>TFHX-FL11</b>	12	2.12	0.005	0.737	1.129	5.16	4867	379	322
	<b>TFHX-FL12</b>	12	2.12	0.005	0.636	1.228	5.16	6681	532	452
	<b>TFHX-FL13</b>	12	2.12	0.005	0.736	1.128	5.16	6681	532	452 / 399
	<b>TFHX-FL14</b>	12	2.12	0.005	0.579	1.285	5.16	9506	765	650
<b>Seawater-seawater</b>	<b>TFHX-FL15</b>	6	3.75	0.005	1.245	2.251	2.53	924	632	537
	<b>TFHX-FL16</b>	14	3.65	0.005	1.690	1.700	5.89	586	478	417
	<b>TFHX-FL17</b>	TBD		0.005	1.509	TBD				
	<b>TFHX-FL18</b>	TBD		0.005	TBD					

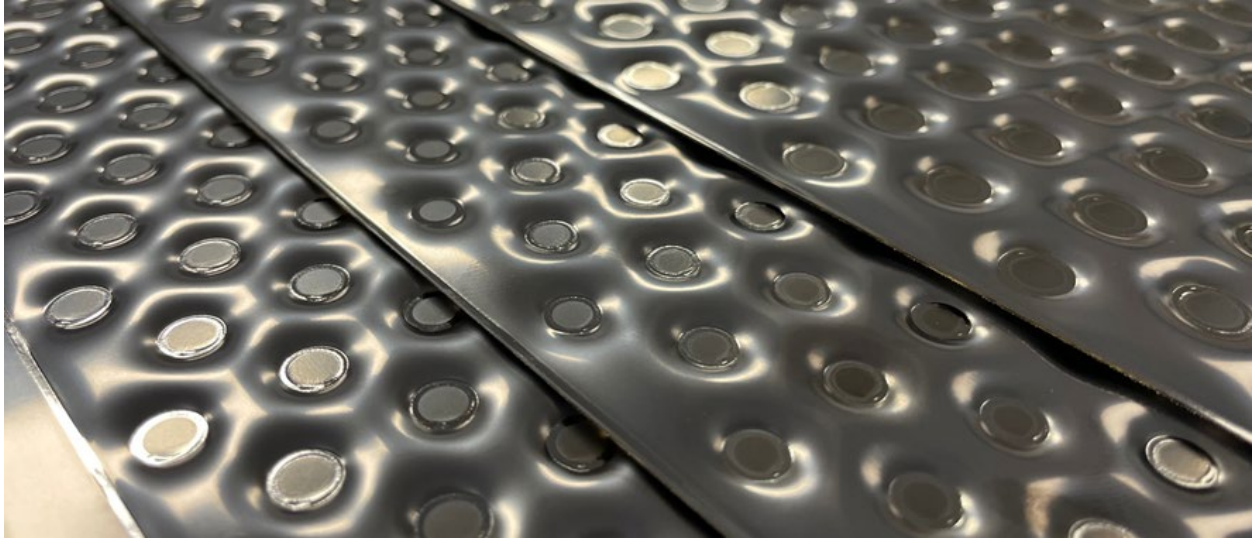


*Figure 8. Seawater-seawater designs with (left to right) 1.7-mm, 1.5-mm, and 1.2-mm effective internal channel sizes.*

## 2.5. PLATE SPACING

### 2.5.1. Seawater Spacers

TFHX performance is dependent on accurate plate spacing so external flow is evenly distributed. Seawater spacers are positioned throughout the plate to ensure the external channels are evenly sized across the entire plate stack. Makai previously selected adhesive backed spacers with a specific durometer and height to stack the cassette-style condenser and evaporator. The spacers were unable to support the weight of the plates in the middle so the stack sags in the middle (Figure 9). Although we expect the sag to go away when the stack is turned on its side in the operational orientation, the sag complicated the stacking process. For the cassette-style evaporator, temporary shims were used to eliminate the sag.

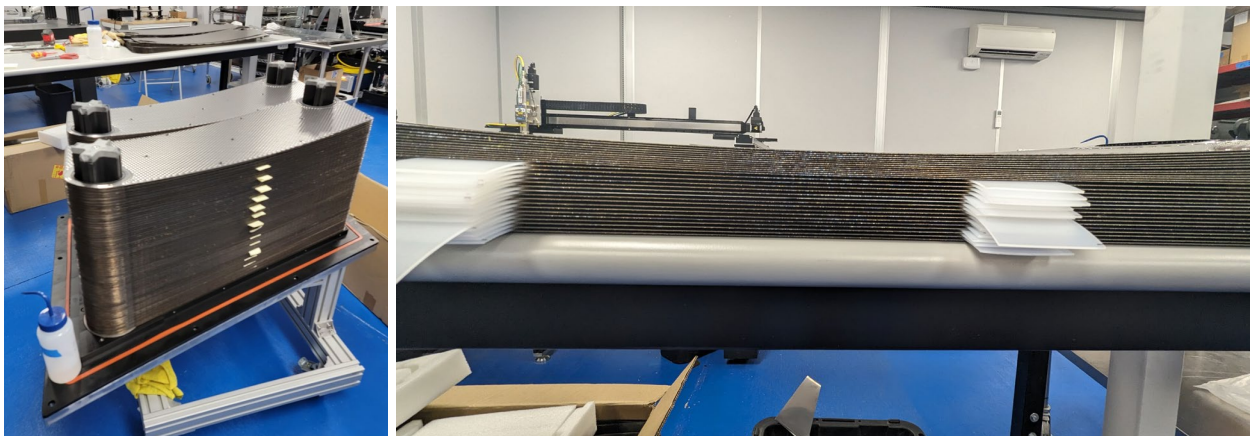


*Figure 9. Seawater spacers could not support the weight of the stack during condenser assembly. Shims were used during evaporator assembly to aid in maintaining even plate spacing during assembly.*

### 2.5.2. Plate Spacing

The seawater cooling applications Makai has been investigating typically have equal internal and external flow rates. The TFHX was originally designed to use refrigerant (ammonia) as the internal fluid, and therefore, internal channel sizes < 1 mm produced acceptable pressure drops. However, when switching to more viscous water/seawater as the internal fluid, the pressure drop was too high for the required flow rate with the small internal channels.

Although Makai can develop patterns to produce larger internal channels, the reduction in pressure drop is also limited by the manifold inlet size and the manifold insert thickness. The insert thickness also sets the plate spacing, which limits the maximum internal channel size. At the existing 2.12-mm plate spacing, the peak-to-peak height of the internal channel is limited to less than ~ 1.8 mm otherwise adjacent plates would touch or compress at the peaks which results in loss of heat transfer area and potentially internal channel size.

Both the manifold size and insert thickness are difficult to modify because the foil forms and weld fixtures are customized to match the manifold size and insert thickness. In order to test the contribution of pressure drop of water through the manifold insert, Makai came up with a way to spiral in a thicker 3D printed insert of the same diameter *after* fabricating a plate with the current insert. The thickest insert that could be spiraled in and seal properly produced a plate spacing of 3.75 mm, which was used in FL-15 and tested in the seawater-seawater configuration. FL-16 was constructed with an insert that produced a 3.65-mm plate spacing and was also tested in the seawater-seawater configuration.

Makai conducted a series of tests to better understand how pressure drop is affected by the pattern, transition, and current manifold design and then compared the empirical data with CFD results. This comparison would help understand CFD analysis of thicker inserts without empirical testing. Four plates were cut to leave about 1" of the pattern weld zone around the manifold and stacked together for the first test (Figure 10). The test sections were then cut again to remove the pattern weld zone but leave the transition zone and re-tested. Finally, the transition welds were removed from each test section and the pressure drop vs flow through the manifold inserts was tested.

For a plate with a 0.52-mm internal channel and **only 1" of pattern length**, the transition and manifold insert contributes about 60% of the total pressure drop (Figure 11). CFD results underpredict the measured pressure drop by about 60%. The actual test plates may have been compressed for sealing purposes (and therefore have smaller passage heights), which is not reflected in CFD analysis. CFD analysis is still useful to compare the relative changes in pressure drop with increased insert thickness. At 3.5-mm plate spacing, the pressure drop through the manifold is predicted to be 1/3 of that at 2.12-mm plate spacing (Figure 12).

In a well-designed plate, the bulk of the pressure drop should occur in the pattern zone where there is heat transfer. With larger internal channels, CFD predicts the existing manifold inserts contribute up to 60% of the total plate pressure drop compared to 30% with thicker inserts. In seawater-seawater testing, for the same pressure drop, Makai was able to double the flow rate through an individual plate by going to a larger internal channel and thicker insert (Figure 13).



Figure 10. (top, left to right). Plates were cut such that flow passed through the (top left) manifold insert + transition + 1" pattern, (top middle) manifold insert + transition zone, and (top right) manifold insert only.

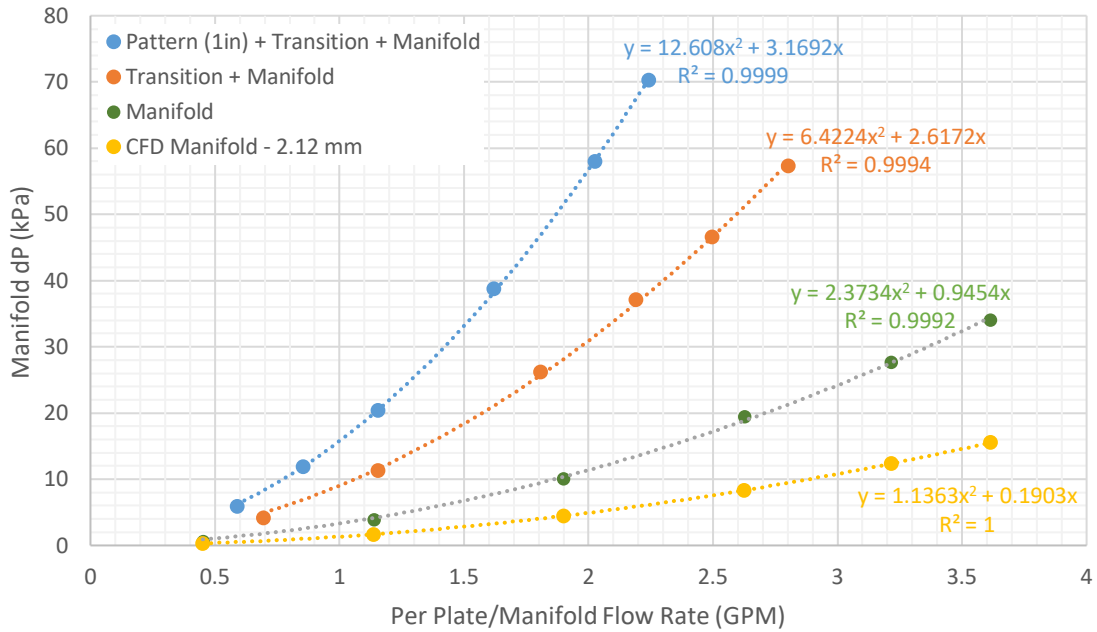


Figure 11. The pressure drop vs flow rate was measured for each of the three configurations. Flow rate is the flow rate through each plate/manifold.

### Measured and Predicted Manifold Pressure Drop

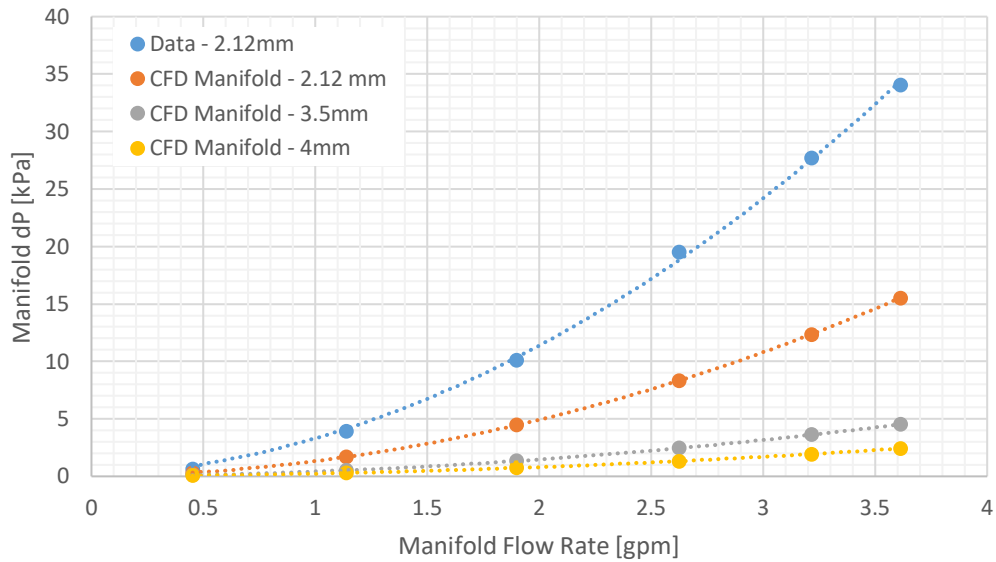


Figure 12. Measured and predicted manifold pressure drop for different plate spacings. 2.12-mm is the current plate spacing.

### Internal Pressure Drop

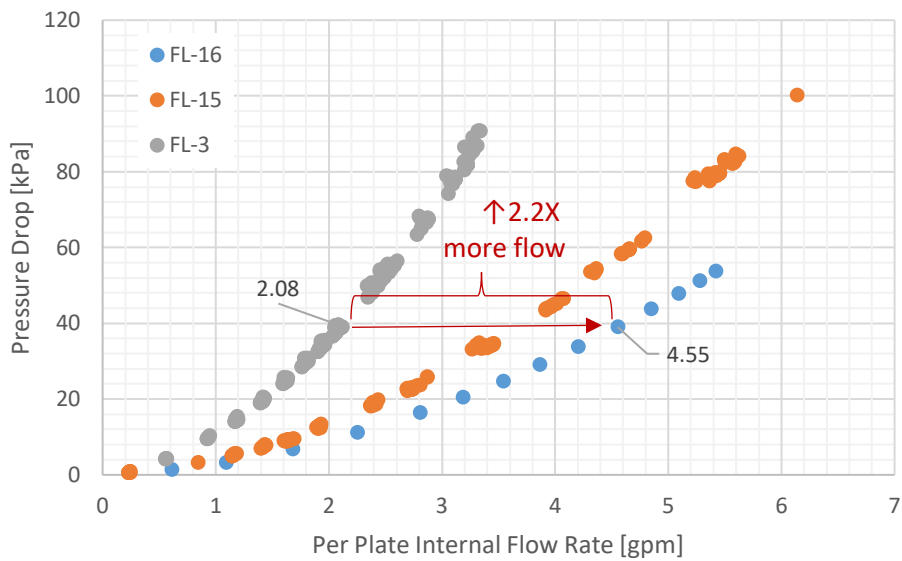


Figure 13. For the same pressure drop, per plate flow rate can be doubled by increasing the internal channel size (from 0.9 mm in FL-3 to 1.70 mm in FL-16) and plate spacing (2.12-mm in FL-9 to 3.65-mm in FL-16, achieved by increasing insert thickness).

## 2.6. HIGH TEMPERATURE HIGH PRESSURE DEVELOPMENT

Makai has been investigating TFHX suitability for high temperature high pressure (HTHP) applications such as concentrated solar power (CSP). Using 0.006" Haynes 230, Makai fabricated a 10-plate prototype unit. The prototype plate design had an > 8,000 psig burst pressure and an effective channel size of 0.21 mm. The test unit was pressurized with CO<sub>2</sub> to between 2000-3000 psig and heated to a maximum temperature of 704°C. After three heat up cycles, a weld failed. Based on the pressure and temperatures the unit experienced, Makai believes the failure mode was creep rupture. Haynes 230 experiences a significant reduction in strength and creep life at temperatures > 600°C.

Makai also experimented with 0.006" Haynes 282, a material that has a lower percentage of temperature-related reduction in strength at temperatures > 650°C and is reported to be more resistant to creep and creep fatigue. We were able to develop weld parameters to join two pieces of Haynes 282 together but the resulting plates had half the predicted burst pressure. We initially suspected the plates required a post-weld heat treatment and purchased a small oven to test out different heat treatment protocols. After experimenting with both solution annealing and age-hardening steps, Makai found no improvement in the weld strength. After discussion with Haynes International, we now suspect the weld parameters require additional development. This work is currently on hold pending alternate funding.

### 3. TFHX FABRICATION AND ASSEMBLY

Makai continues to focus fabrication efforts on improving efficiency and success rates to achieve fast, reliable, repeatable, high-quality TFHX plates and complete heat exchanger units. This includes revisions to improve existing equipment and fixturing and tooling and methods to improve weld quality control and repair.

In this period, Makai focused on:

- Troubleshooting plate failures and identifying fixturing-related issues,
- Improving quality control methods,
- Evaluating new sealing methods,
- Optimizing parameters to reduce plate fabrication time.

#### 3.1. PLATE FABRICATION IMPROVEMENTS

In this period, Makai constructed two 300-plate TFHXs and was able to achieve 80-90% plate success rates over a series of 50+ plate fabrication runs. The high-volume fabrication enabled us to identify, analyze, and adjust factors the influence success rate.

#### 3.2. WELD DEFECT IDENTIFICATION AND REPAIR

Makai also made modifications to the weld defect detection algorithm and improvements to the lighting system. In the first post-adjustment run, the initial success rate (which includes automatic defect detection and patching) was 117 out of 149 plates (79%) of plates were good. An additional 18 plates were successfully patched manually, bringing the overall number of good plates to 135 out of 149 (90%). On average, there were 1.5 auto-patches per plate. On the 50-plate run prior to implementing the quality control improvements, only 28% of the plates were initially successful and overall 64% were successful after manual patching. The improvements to the lighting and detection algorithm, in addition to increased skill in the wiping process, likely contributed to the substantial increase in initially successful plates. Post-expansion or manual patching is effective, but time consuming; therefore, higher initial success rates are heavily favored.

One drawback to the existing system is that the imaging also uses the scanhead, which means, there must be a delay for the welds to cool before welds can be imaged. This artificially increases the weld time. Makai will be testing a new, separate camera system that is faster and has independent control and processing capabilities. This new system will also be able to evaluate and automatically repair seal weld defects which currently relies on manual inspection and patching. This new system is expected to reduce the current weld and imaging step time by a factor of 3. Although waiting to image the plate after all welding is complete risks not catching cascading failures in time to save a plate, cascading failures have become increasingly rare with proper foil handling and installation and the advantages gained by separating welding from imaging are worth exploring.

### 3.3. PRODUCTION RUN STATISTICS

Production runs were done on cassette-style plates with two different patterns, a wobble weld pattern for the condenser and a dot pattern for the evaporator. The condenser plate design had 2940 wobble welds per plate whereas the evaporator plate design had had 7513 dot welds per plate.

Makai previously reported that the initial success rate for the first 107 plates of the condenser was 49% with manual patching bringing the overall success rate up to 69%. There was significant inconsistency observed over the 4-day fabrication run, with overall success rates decreasing from 82% on Day 1 to 25% on Day 4. The next 62 plates yielded similar results, 26% initial success rate and 60% overall success rate after manual patching (Table 2). After making improvements to the lighting and auto detection algorithm, the next 149 condenser plates had an initial success rate of 79% and overall success rate of 90% after manual patching. Similar results were observed for evaporator plates (Runs 3-5 on Table 2). Experience gained over practicing the wiping process to remove air bubbles between the foils also likely contributed the improvement in initial and overall success rates.

*Table 2. Production Statistics*

	Run 1	Run 2*	Run 3	Run 4*	Run 5*
Pattern	Wobble	Wobble	Dot	Dot	Dot
Plates attempted	62	149	70	96	81
Initial good plates	16	117	41	72	67
Initial success rate	26%	79%	58%	75%	83%
Successful manual patch plates	21	18	14	7	5
Failed patches/ Un-patchable	25	14	7	17	9
Overall success rate	37 out of 62 (60%)	135 out of 149 (90%)	55 out of 70 (79%)	79 out of 96 (82%)	72 out of 81 (89%)

### 3.4. FUTURE AREAS OF FOCUS

Makai has been working on plans for the next iteration of the HSW. With repeated demonstrations of fabrication success rates > 80%, Makai intends to improve on the current formed foil method by:

- Forming in-house to control cleanliness, storage, eliminate damage from shipping, reduce cost
- Designing new fixtures

- Adding scanheads in parallel to speed up weld time
- Adding independent imaging equipment to speed up weld time
- Improvements to argon plenum to save on argon usage
- Separating welding from expansion equipment to speed up plate cycle time

## 4. TFHX PERFORMANCE TESTING

In this period, Makai built 3 stand-alone 100-kW scale TFHX units with different internal/external channels and plate spacings (Table 3). One unit was tested in a counterflow configuration as an evaporator and briefly as a condenser (Figure 14). Condenser testing was not completed due to a recirc pump failure at the 100-kW Test Station. The other two units were tested in a counterflow configuration using cold seawater as the internal fluid and warm seawater as the external fluid. As reported previously, Makai also built two 2-MW scale TFHXs for testing once upgrades to the HX Facility are complete and the HX Facility is commissioned.

*Table 3. Overview of TFHX test units.*

	# Plates	Plate Spacing [mm]	Foil Thickness ["]	Internal Channel Size [mm]	External Channel Size [mm]	Fluid Length [m]	HX Area [m <sup>2</sup> ]
<b>TFHX-FL14</b>	12	2.12	0.005	0.579	1.285	0.86	5.16
<b>TFHX-FL15</b>	6	3.75	0.005	1.245	2.251	0.86	2.58
<b>TFHX-FL16</b>	14	3.64	0.005	1.690	1.700	0.86	6.02

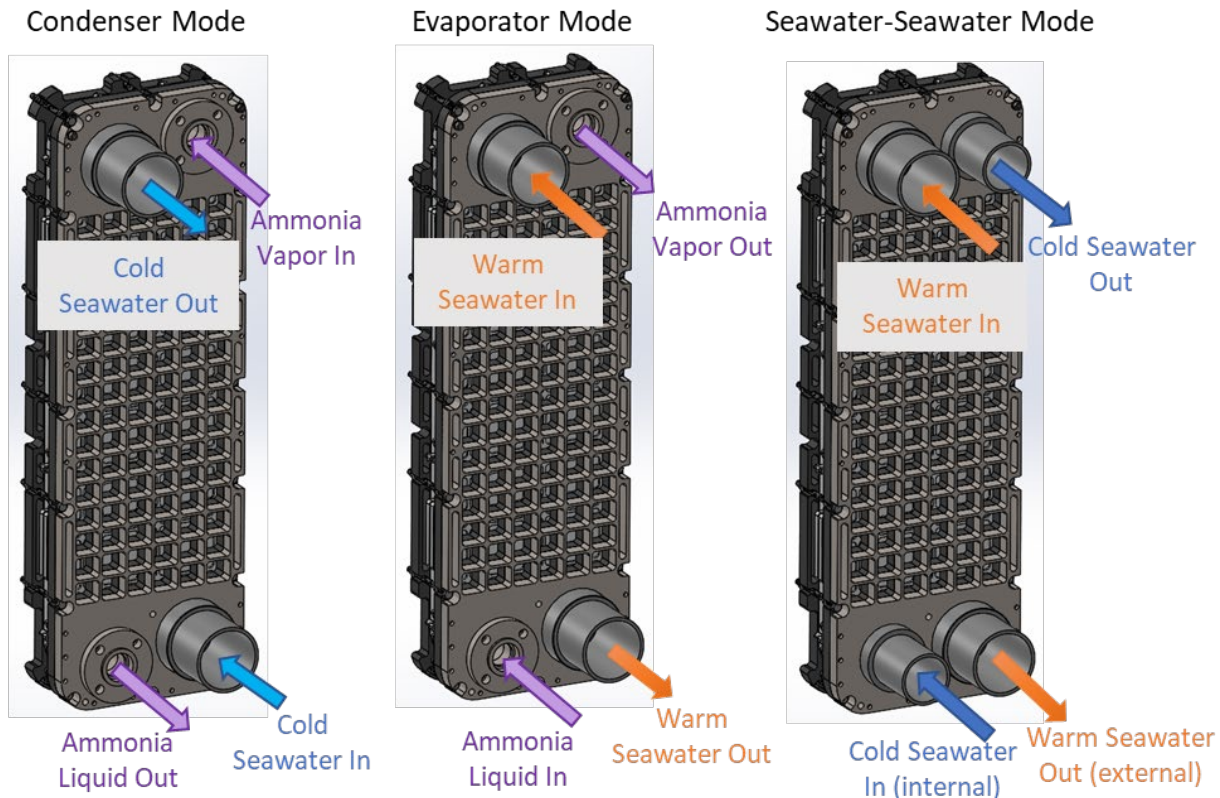


*Figure 14. Full-length TFHX module configured for counterflow condenser, evaporator, and seawater-seawater testing.*

TFHX-FL14 was part of a series of THFXs with pattern weld designs were specifically selected to have incremental changes in internal channel size (TFHX-FL11, -FL12, and -FL14) for comparison with previous performance testing data.

TFHX-FL15 and -FL16 were designed for water as the internal fluid with larger effective internal channels and thicker manifold inserts to allow more flow into each plate.

#### 4.1. 100-KW TEST STATION OPERATIONS

In this period, Makai replaced all relief valves at the 100-kW Test Station to prevent inadvertent ammonia releases. FL14 was tested as an evaporator first and then switched to condenser testing. After a few condenser test points, the recirculation pump seized and we were unable to pump ammonia. The motor was verified functional but the pump shaft could not be rotated by hand. The most likely cause is some debris binding the pump. The pump is at the lowest point of the system which is full of liquid ammonia and cannot be isolated for repairs without first moving the ammonia into the buffer tank (by condensation). Maintenance is scheduled for after the HX Facility upgrades for 2-MW TFHX testing is complete.

#### 4.2. HX FACILITY UPGRADES

Under separately funded work, Makai has been upgrading the HX Testing Facility in preparation for 2-MW TFHX testing. All Lockheed shell and tube heat exchangers have been removed from the facility and remaining APV and CHART heat exchangers are no longer connected to the new ammonia piping system. The facility was redesigned with safety features used in the 100-kW Test Station; most of the ammonia system (e.g., piping, tanks, and pumps) is contained in two enclosures (buffer and separator) equipped with atmospheric ammonia detectors, ventilation, and deluge. Only the TFHXs and piping connecting the evaporator and condenser sides are outside the enclosure.

To minimize effort required to maintain carbon steel piping free of corrosion, all new ammonia piping is stainless steel. The feed and recirculation pumps are higher capacity versions of those used in the 100-kW system. With gear pumps, ammonia flow is controlled solely through VFDs rather than both VFDs and a network of bypass and control valves that was required with the previous centrifugal pumps. Two expansion valves, one for coarse and the second for fine control, are used in place of a turbine to drop pressure between the evaporator and condenser. Seawater flow rates are controlled using the existing 18" butterfly control valves (coarse control) and newly 6" butterfly control valves (fine adjustment). The previous data acquisition and control hardware was also replaced with a new Compact RIO system to meet updated network security requirements.

Facility commissioning is planned for December 2024.

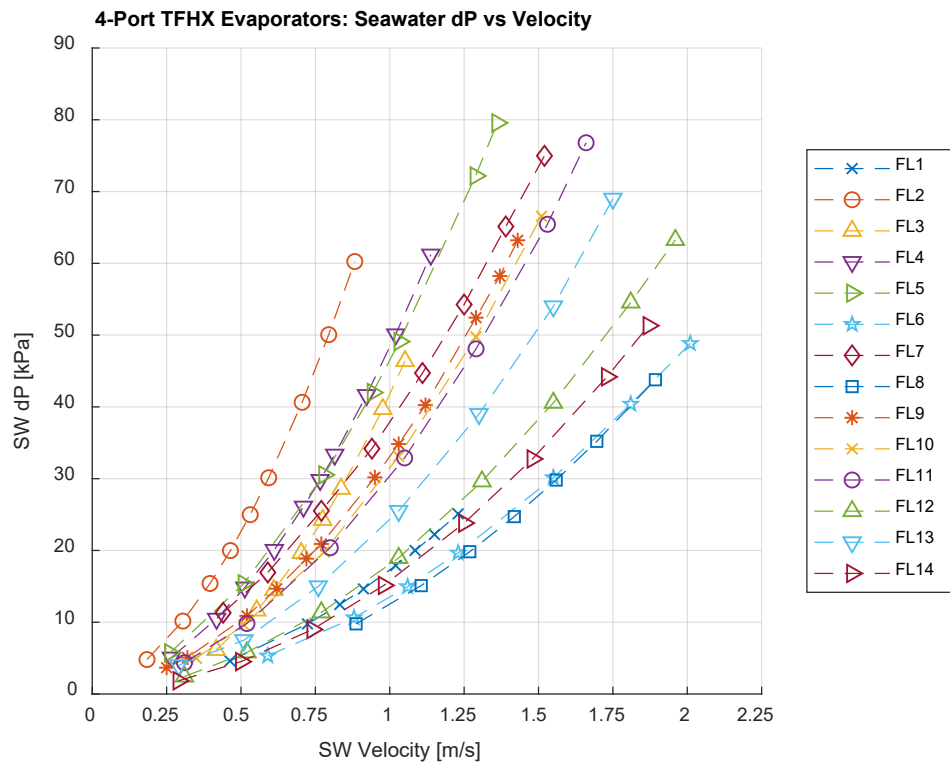
#### 4.3. SEAWATER-AMMONIA PERFORMANCE TESTING

TFHX-FL14 was tested as an evaporator at energy densities between 5-20 kW/m<sup>2</sup> and seawater velocities between 0.3-1.8 m/s. As a condenser, only energy density of 7.5 kW/m<sup>2</sup> was tested prior to recirc pump failure. Ammonia duty was controlled by controlling the seawater flow rate through

the companion (APV) heat exchanger and use of the expansion valve. For example, during evaporator testing, the APV heat exchanger functions as a condenser; increasing the cold seawater flow through the APV increases TFHX duty at a fixed TFHX seawater flow rate. Seawater flow was controlled by adjusting seawater control valves. During evaporator testing, the quality is set by adjusting the ammonia liquid flow rate using a VFD to control the feed pump.

#### 4.3.1. Seawater Pressure Drop

Seawater-side pressure drop is related to the pumping power required to provide a certain seawater flow rate through the heat exchanger. The seawater pressure drop is mainly dependent on channel size and seawater velocity (Figure 15). At the same velocity, the pressure drop when tested as an evaporator versus a condenser should be comparable. Some plate designs exhibit limited expansion/contraction of the internal channel size with differences in internal vs external pressure and small deviations in pressure drop between evaporator and condenser mode are expected.



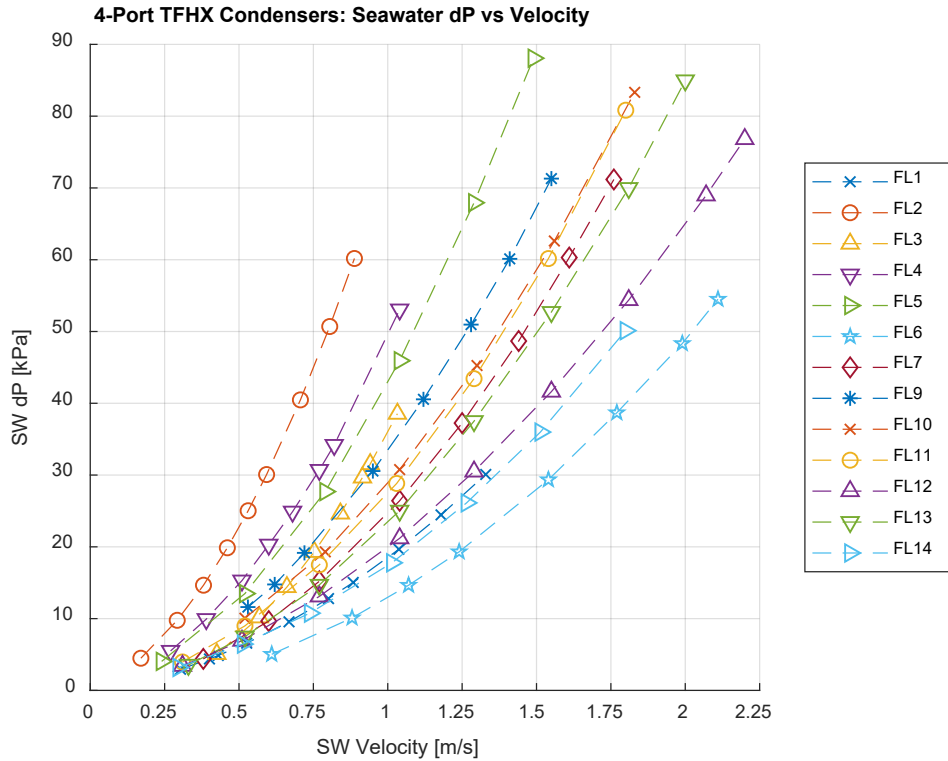


Figure 15. Seawater pressure drop for all tested TFHX units.

#### 4.3.2. Ammonia Pressure Drop

Ammonia-side pressure drop is an important consideration for an evaporator/condenser. In a closed-cycle OTEC system, minimizing the pressure drop increases the available differential pressure across a turbine and reduces the pumping power required to recirculate refrigerant. Ammonia pressure drop is strongly dependent on ammonia vapor flow rate, quality, and heat exchanger geometry.

Ammonia-side pressure drop versus energy density is shown for 12-plate TFHX units to minimize the effect of manifold duct losses and focus on the effect of internal channel size and pattern weld design (Figure 16). TFHX-FL10 through -FL14 used the same weld diameter at different weld spacings to produce effective internal channels from 0.58 mm to 0.84 mm. TFHX-FL13 and -FL11 had the same effective internal channel size but used a different weld spacing and expansion pressures. TFHX-FL3 and -FL5 had the same weld diameter and weld spacing but different expansion pressures to produce effective internal channel heights of 0.90 mm and 0.78 mm.

In both evaporator and condenser configurations, designs with the largest effective internal channel heights had the lowest pressure drop at the same energy density. For the same effective internal channel height, TFHX-FL13 had a tighter weld spacing compared to TFHX-FL11 and slightly higher pressure drop.

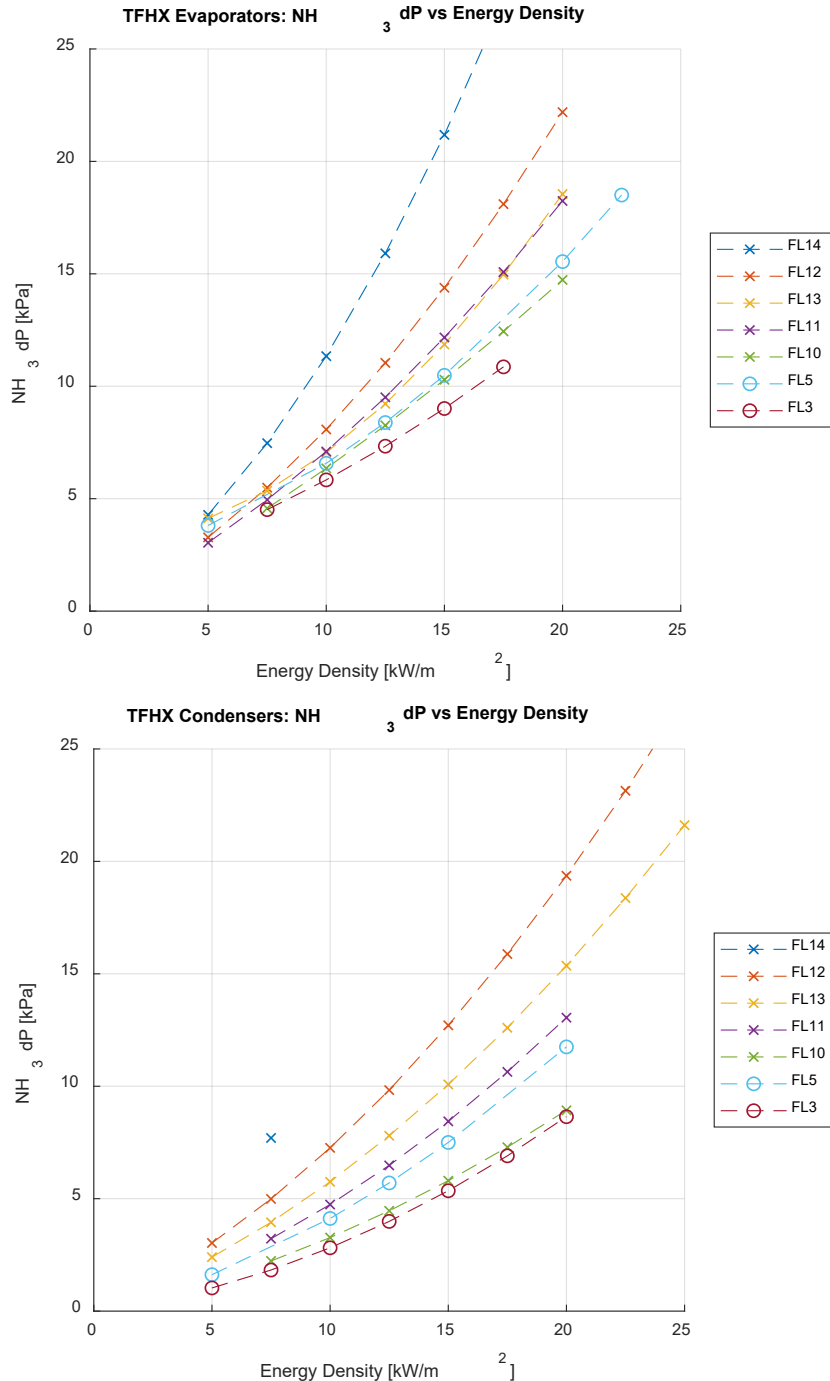


Figure 16. Ammonia pressure drop versus energy density for 12-plate TFHX units.

#### 4.3.3. Overall Heat Transfer Coefficient

U-value is predominantly dependent on seawater flow rate but duty (and quality for an evaporator) also has an effect. U-values increase almost linearly with increasing seawater flow (Figure 17) over the range of the tested velocities. As an evaporator, at higher seawater velocities, a slight decrease in U value is observed when increasing energy density from 12.5 kW/m<sup>2</sup> to 20 kW/m<sup>2</sup> (Figure 18).

TFHX Designs with 1.15 mm Weld Diameters

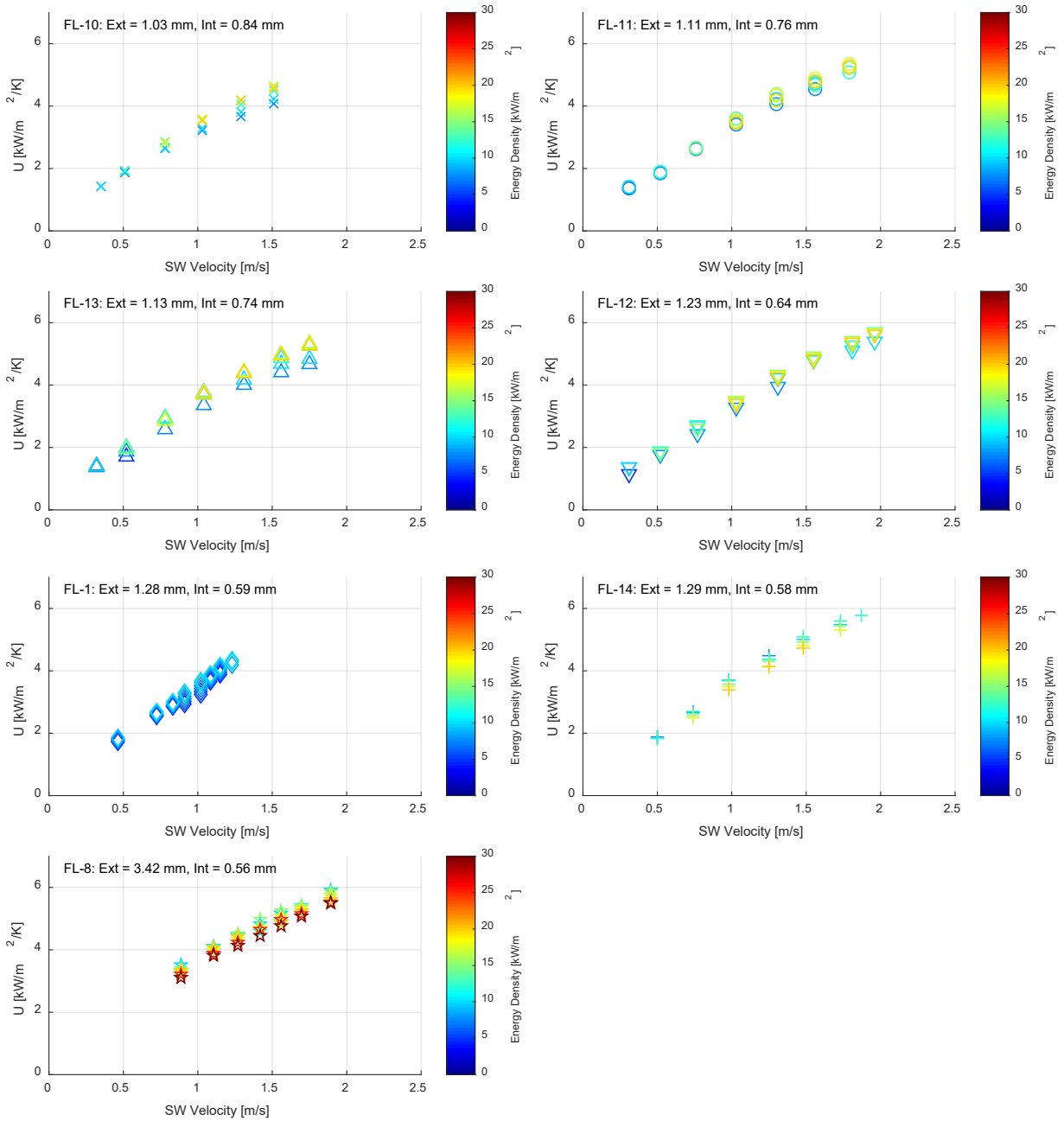


Figure 17. U-value vs seawater velocity.

TFHX Designs with 1.15 mm Weld Diameters

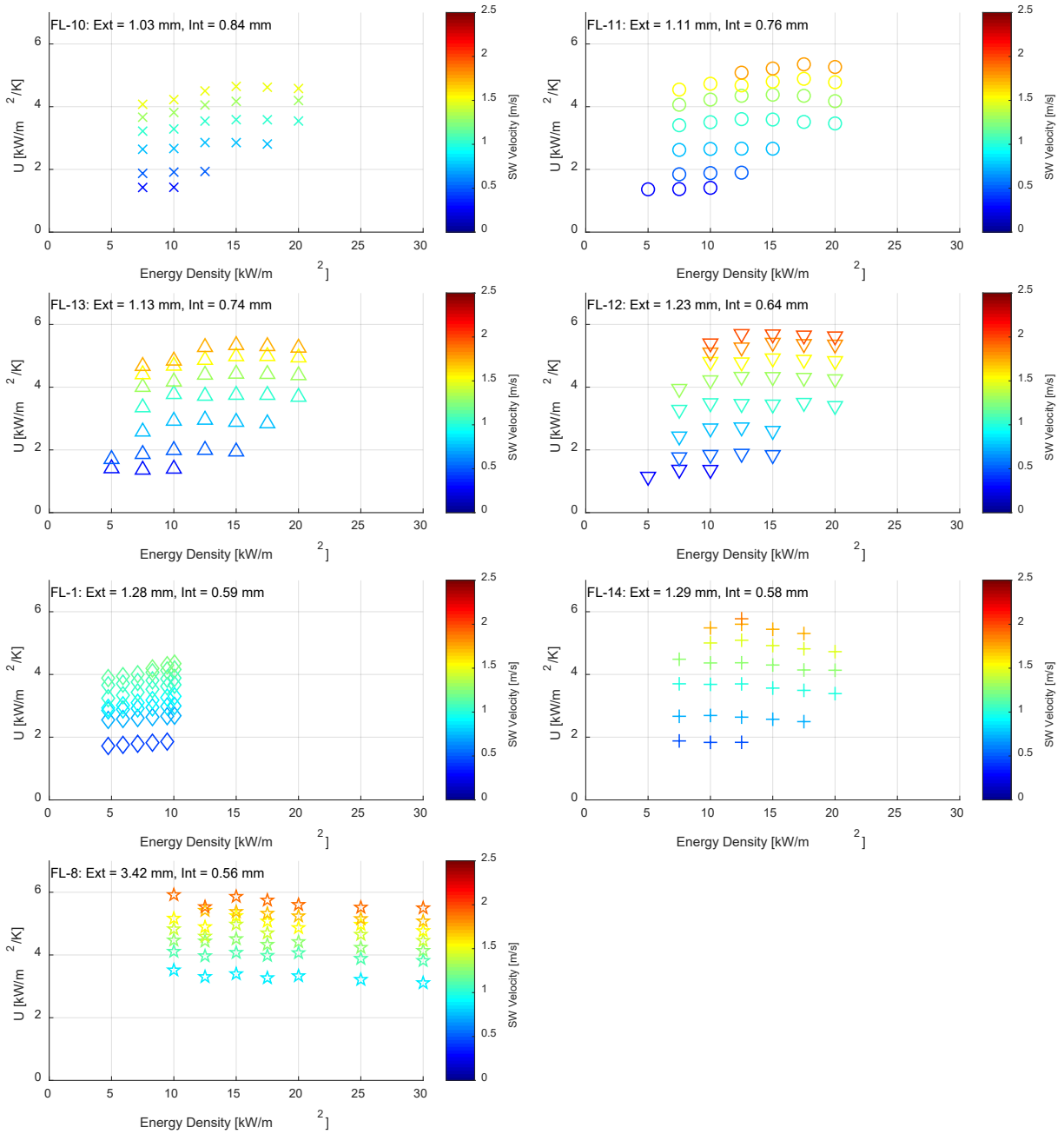
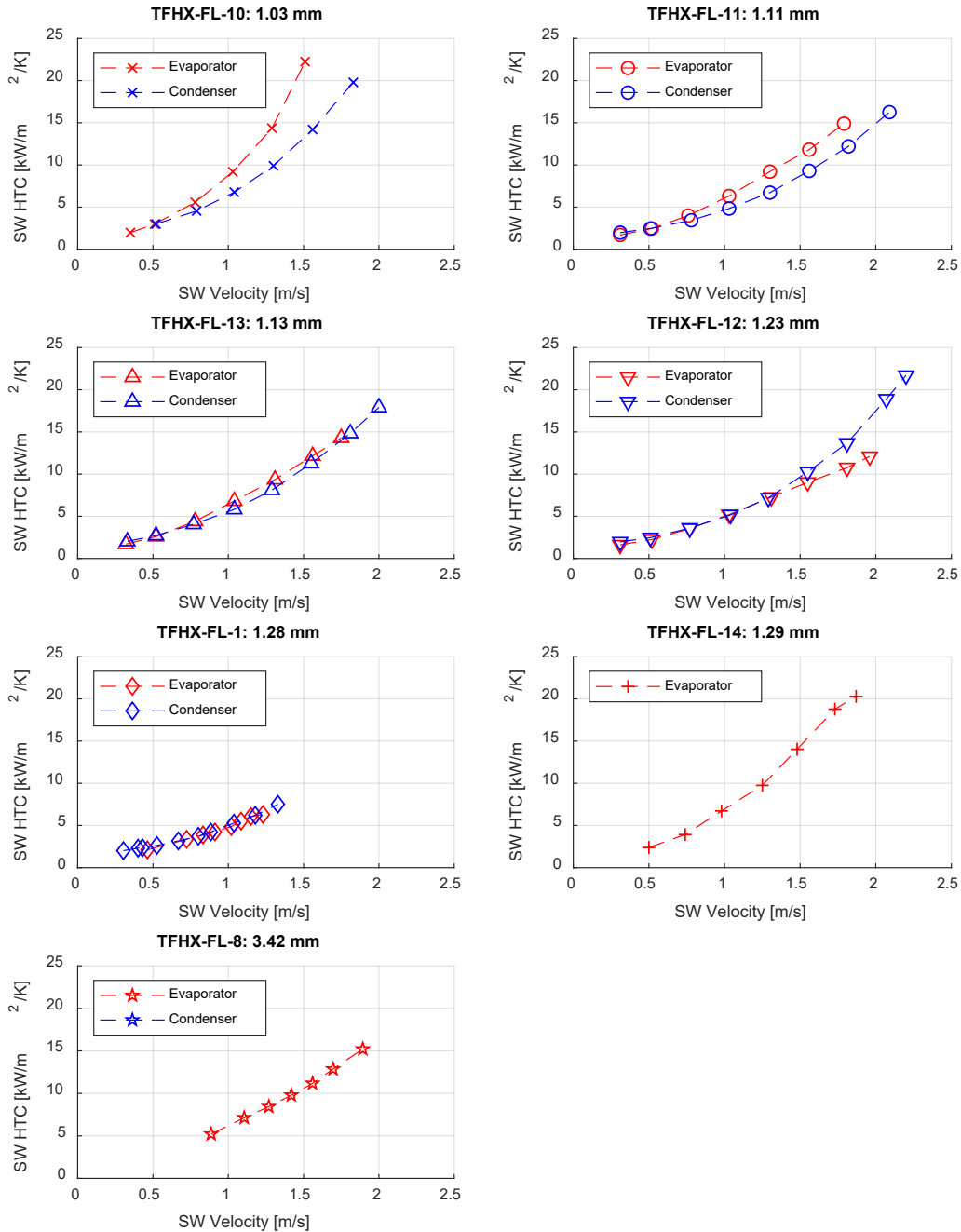


Figure 18. U-value vs energy density.

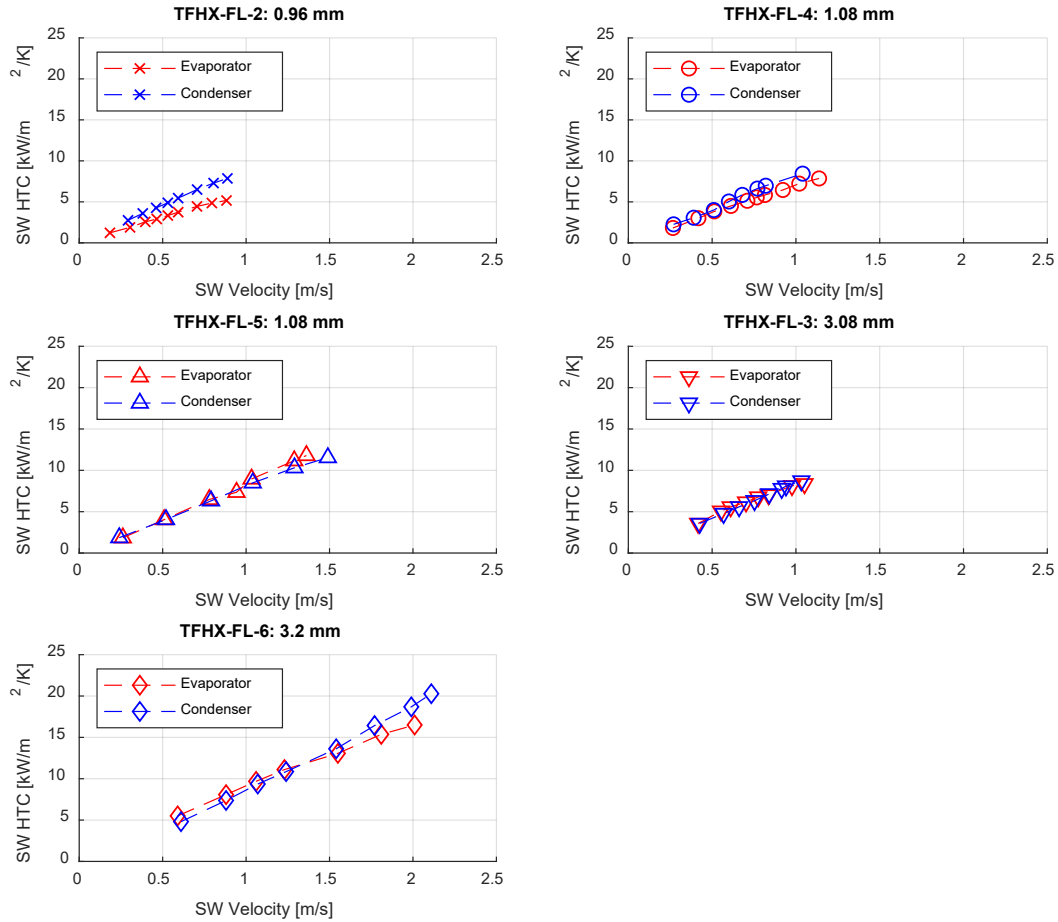
4.3.4. Convective Coefficients

Makai previously reported that there is substantial uncertainty surrounding convective coefficients due to mathematical limitations of solving equations where there are more unknowns than equations and the effects of averaged versus localized heat transfer performance.

Seawater side convective coefficients were solved independently for each configuration (condenser or evaporator) for each TFHX unit. FL-14 is shown with previously tested designs using the same weld design (Figure 19). Unlike designs with the different weld designs (Figure 20), seawater convective coefficients increase non-linearly with increasing seawater velocity.

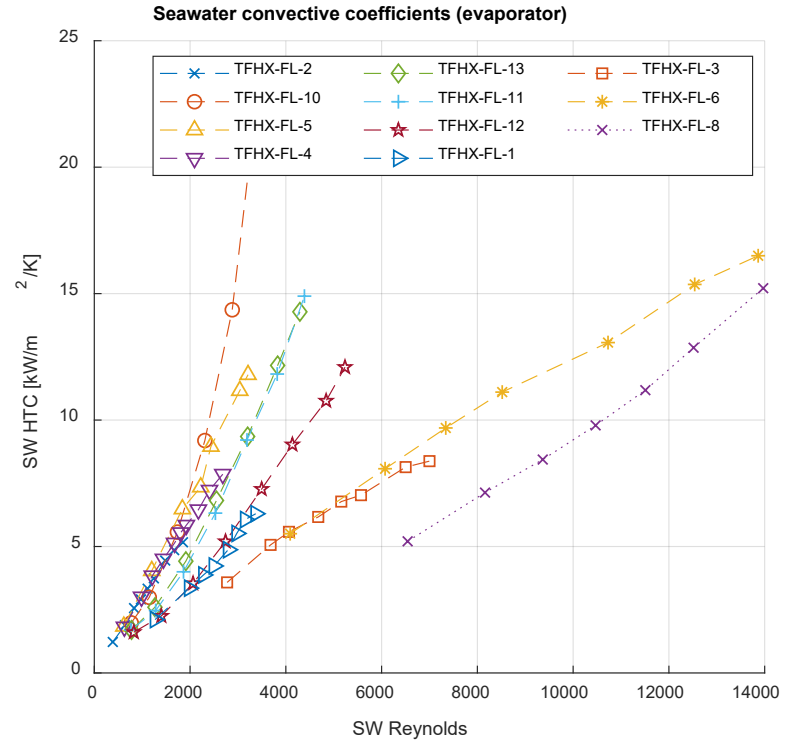
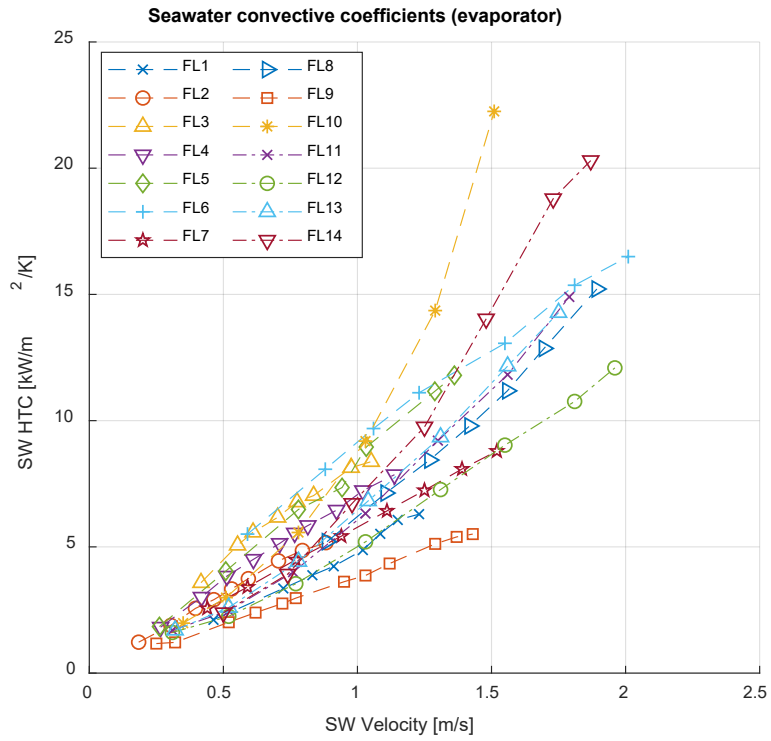


*Figure 19. Seawater-side convective coefficients for TFHX units with pattern weld designs using the same weld but different weld spacings and expansion pressures. External channel size is shown after the unit number.*



*Figure 20. Seawater-side convective coefficients for TFHX units with the same pattern weld design but different expansion pressures. External (seawater) channel size is shown after the unit number.*

There is no clear trend between heat exchanger channel size and seawater convective coefficients vs. velocity (Figure 21). Heat exchangers with large seawater channels (FL-3 and FL-6) had among the highest seawater convective coefficients for the same velocity, but FL-8, which also had large seawater channels had lower seawater convective coefficients compared to heat exchangers with smaller seawater channels such as FL-5. Heat exchangers with comparable channel sizes had comparable convective coefficients at the same Reynolds number. For the same pressure drop, heat exchangers with larger channels had higher convective coefficients. For the same pumping power (represented by flow rate times pressure drop), there is no trend for convective coefficients and channel size. The smallest seawater channel (TFHX-FL2) had the lowest convective coefficient for the same pumping power. However, the largest channel sizes (TFHX-FL3 and -FL8) had the next lowest convective coefficients.



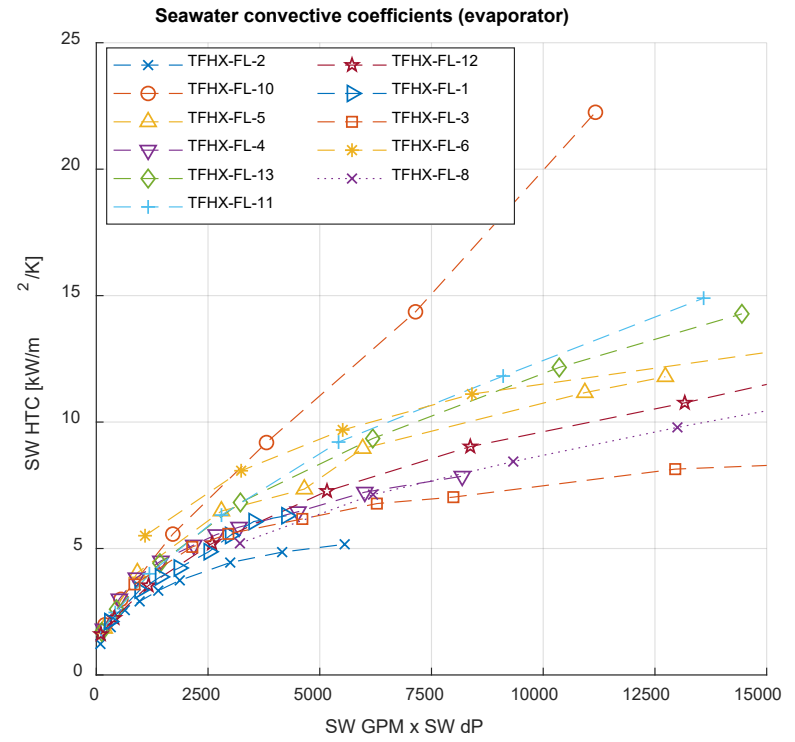
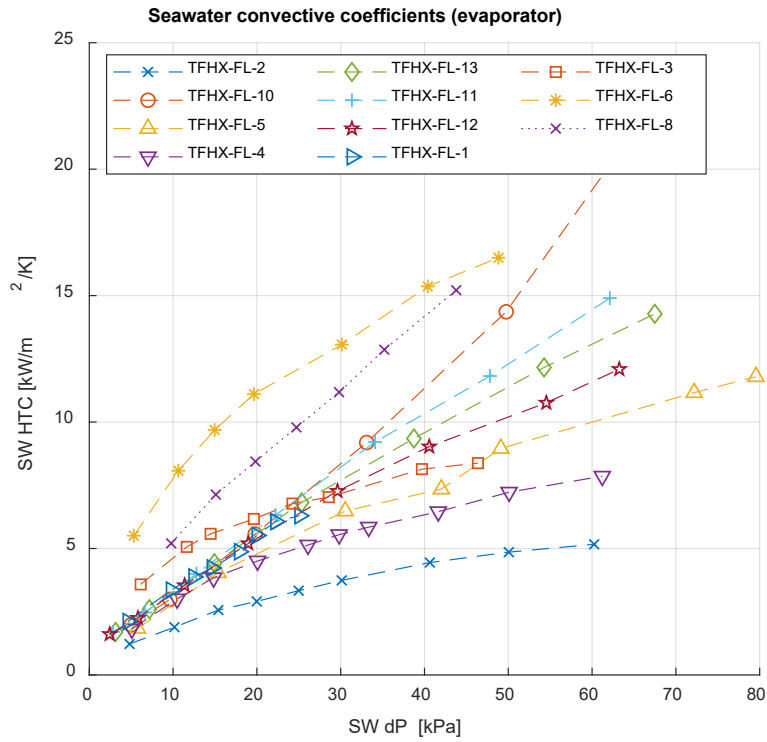
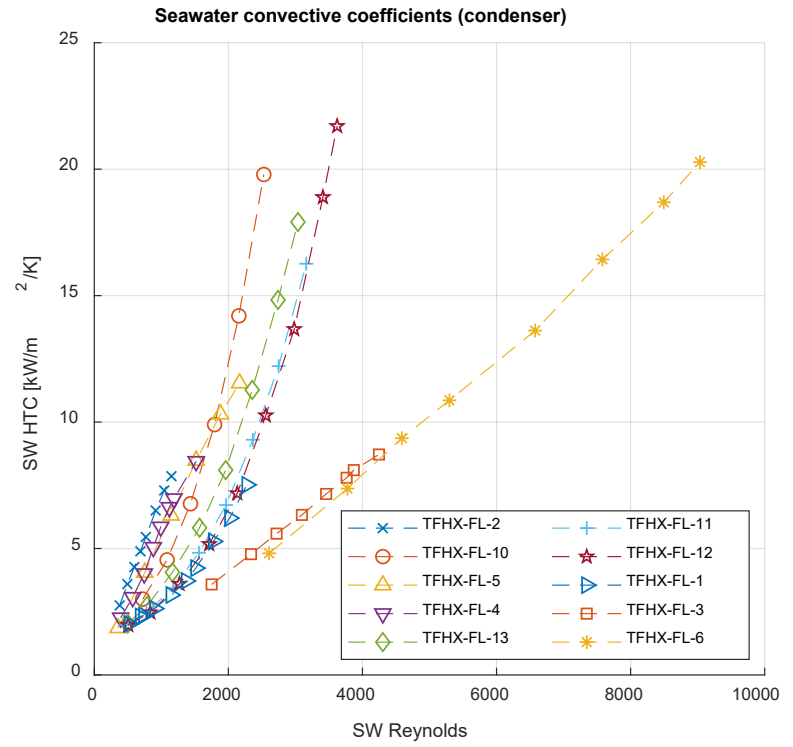
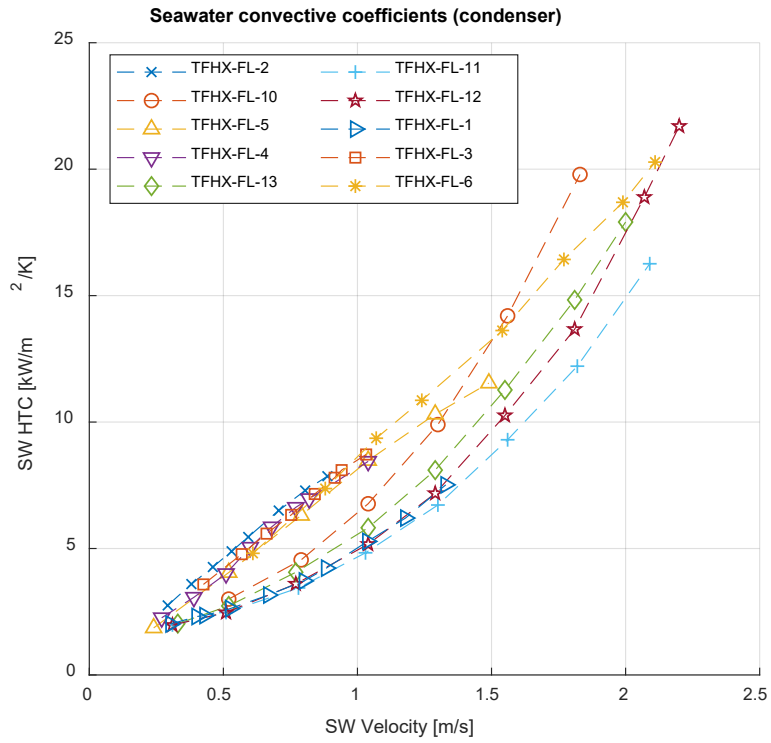


Figure 21. Evaporator seawater convective coefficients. TFHX units are listed from smallest seawater channel (TFHX-FL2) to largest (TFHX-FL8)



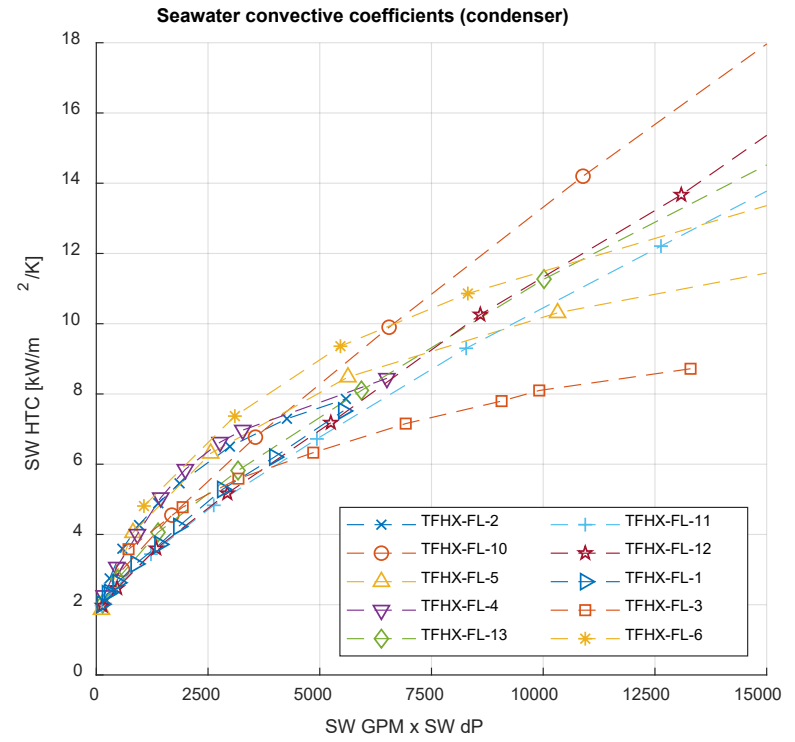
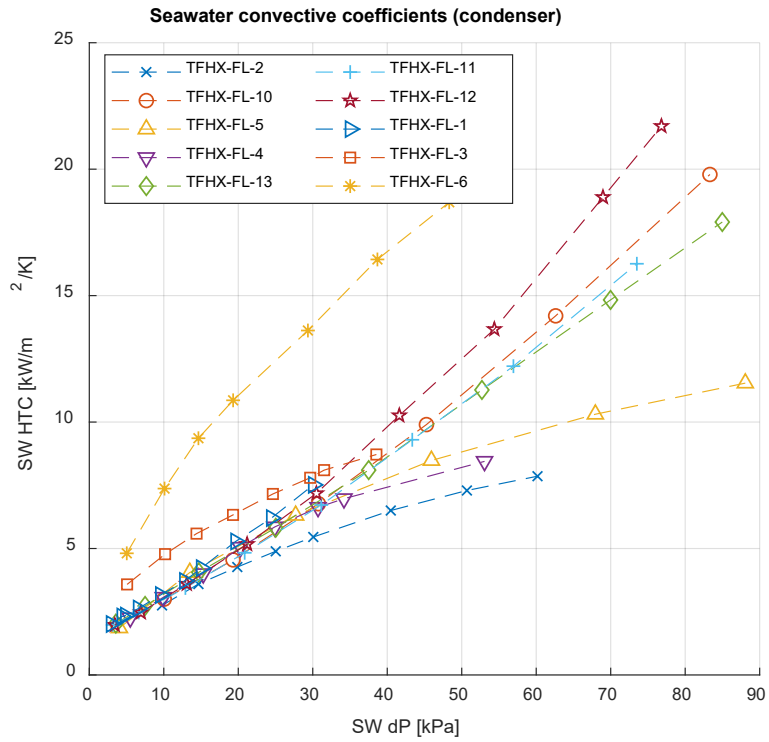
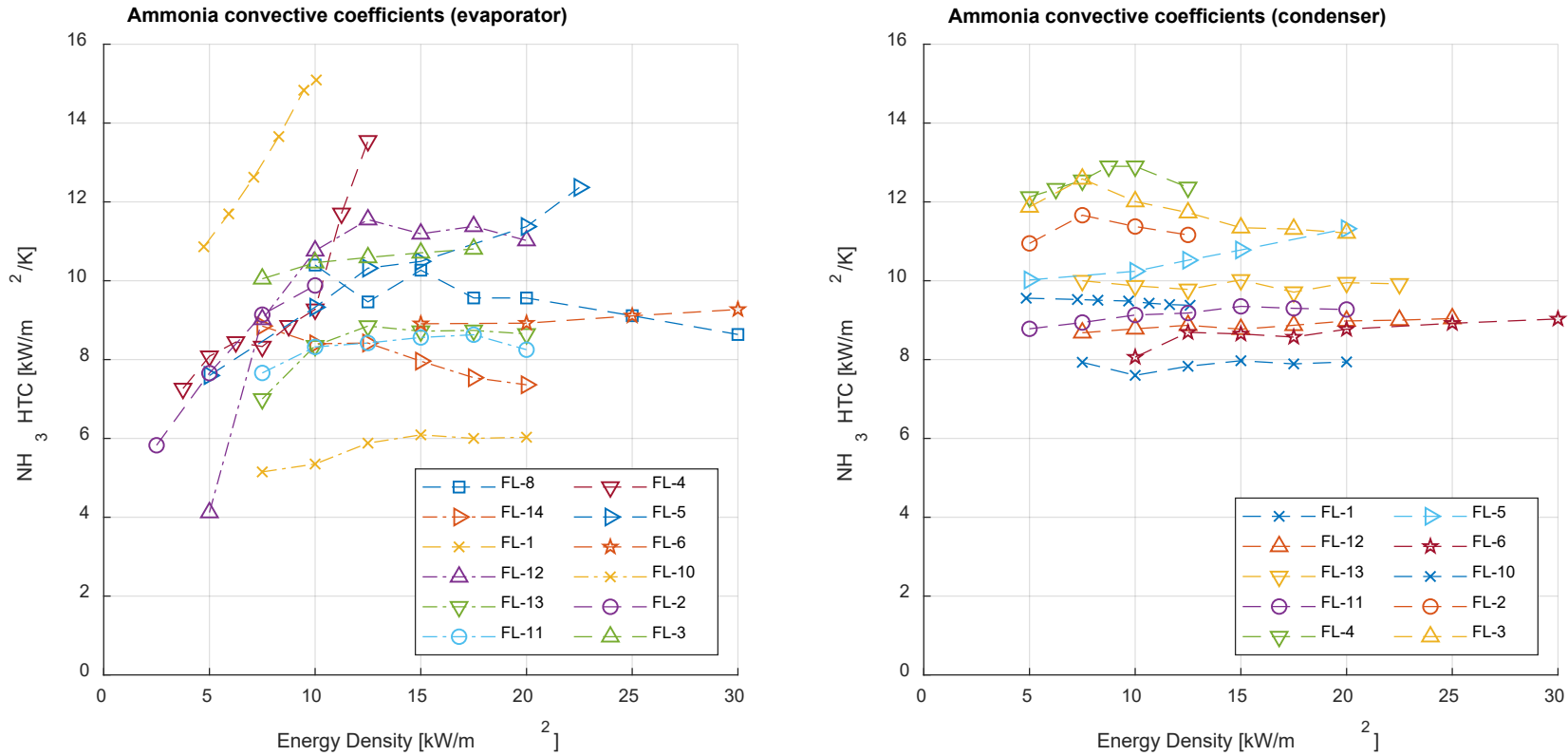


Figure 22. Condenser seawater convective coefficients. TFHX units are listed from smallest seawater channel (TFHX-FL2) to largest (TFHX-FL6)

*Ammonia side convective coefficients.*

Ammonia-side convective coefficients also did not have a clear trend with ammonia channel size (Figure 23). In general, ammonia convective coefficients increase with increasing energy density up to 10 kW/m<sup>2</sup> and decrease at higher energy densities.



**Figure 23. Ammonia-side convective coefficients for evaporator and condenser. TFHXs are listed from smallest ammonia effective channel (TFHX-FL8/-FL1) to largest (TFHX-FL3).**

#### 4.3.5. Heat Exchanger Approach Temperature

Heat exchanger approach temperature is determined by the seawater temperature, seawater flow rate, and duty. Makai is defining the approach temperature as:

$$T_{approach} = T_{warm\ seawater\ in} - T_{saturation\ at\ EOPS} \text{ (evaporator)}$$

$$T_{approach} = T_{saturation\ at\ CIPS} - T_{cold\ seawater\ in} \text{ (condenser)}$$

Makai's definition is customized for OTEC purposes; the ammonia saturation temperatures at the evaporator outlet and condenser inlet are used because these are directly connected to the turbine inlet/outlet. Additionally, because the bulk of the duty is in phase change, superheating at the condenser inlet is not accounted for and the saturation temperature is used instead of the measured temperature.

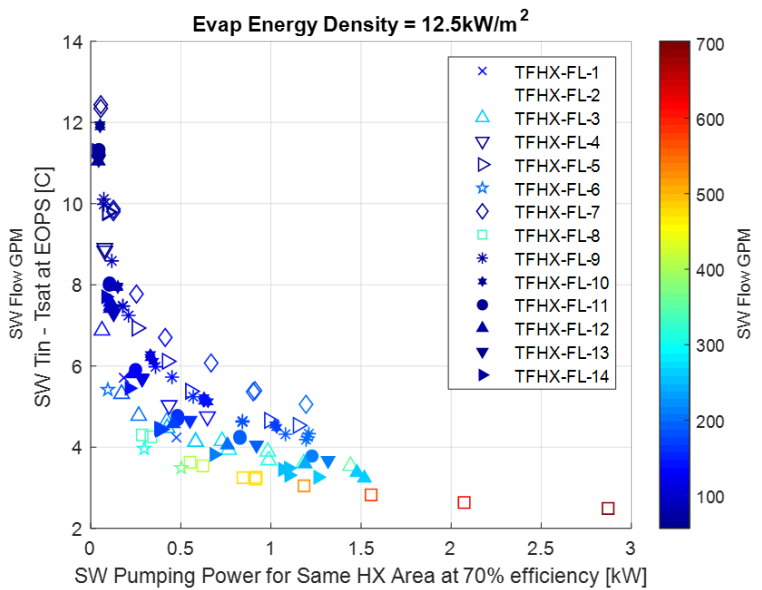
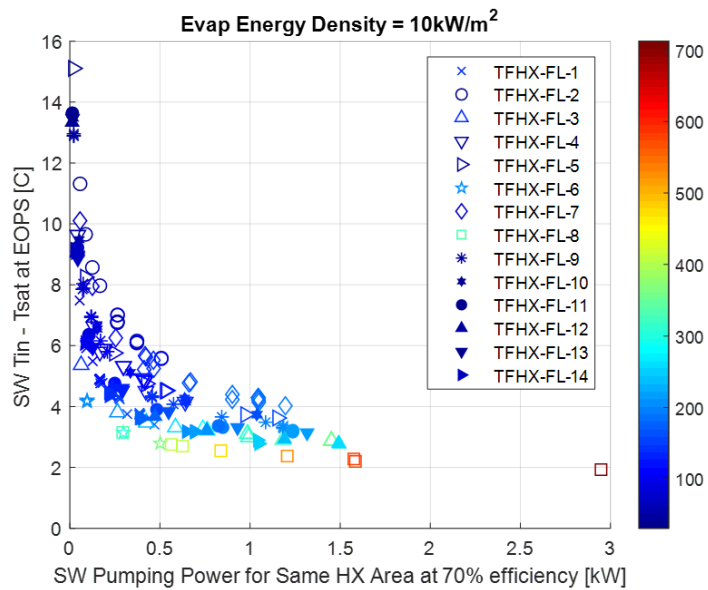
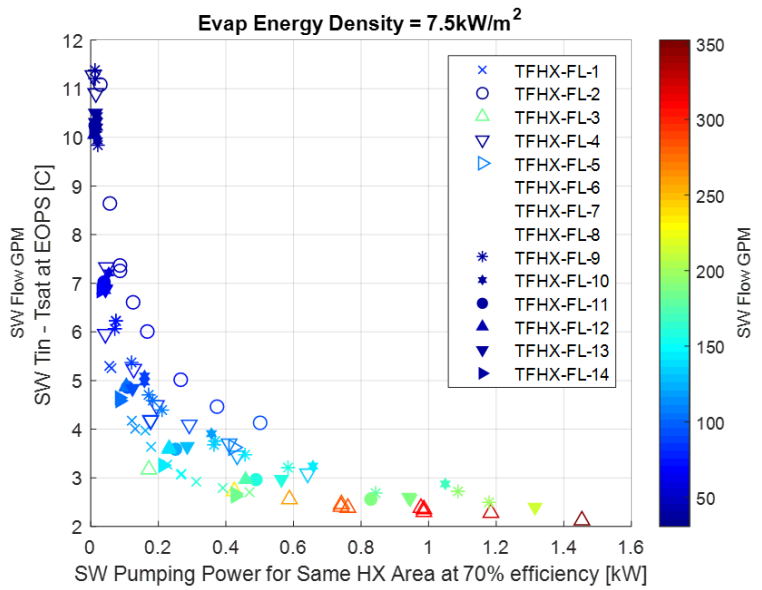
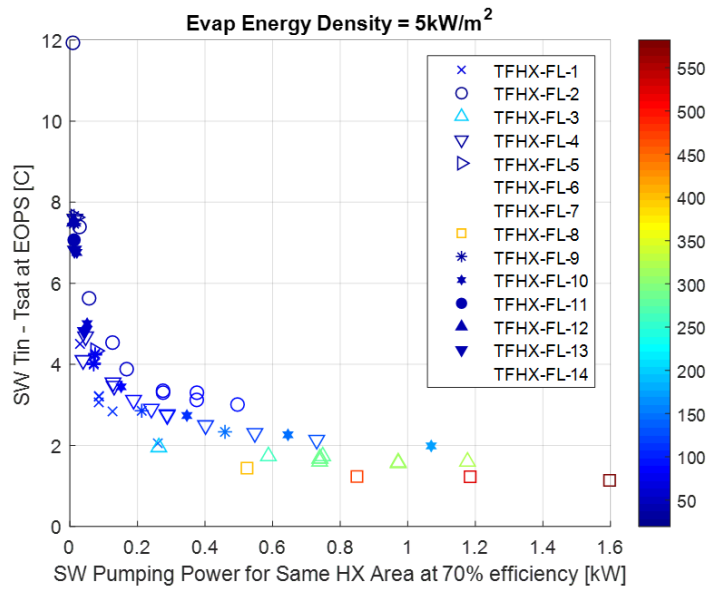
For OTEC operations, small approach temperatures result in higher available differential pressure across the turbine. Higher seawater flow rates yield smaller approach temperatures, but also require higher parasitic losses from high volumetric flow rates and/or high seawater pressure drops.

One way to compare heat exchanger performance is to match heat transfer areas and then compare the approach temperature versus pumping power at fixed energy densities (Figure 24 and Figure 25).

For both evaporator and condenser modes, TFHX units with 4.24-mm plate spacings (FL-3, FL-6, and FL-8) and, therefore, larger seawater channels, had the lowest approach temperatures for the same pumping power. FL-1 and FL-12 had the lowest approach temperatures of the TFHX units with 2.12-mm plate spacing and also had comparable approach temperatures compared to FL-3.

This analysis only considers the pumping power through the heat exchanger. For OTEC operations, the total volume of seawater flow is also important, particularly for the condenser. For example, although FL-3 and FL-6 had the lowest condenser approach temperatures, the both required up to 2.5X the flow as FL-4. Furthermore, at the same pumping power, FL-4 had 10% higher approach temperature than FL-1 but used 20% less volumetric flow. For a fixed cold water pipe size, lower volumetric flow rates have lower seawater system losses.

A comprehensive comparison of TFHX designs in the OTEC context will require a tradeoff study evaluating increase in net power production gained by smaller approach temperatures versus a larger cold water pipe and overall OTEC system (i.e., more expensive capital investment).



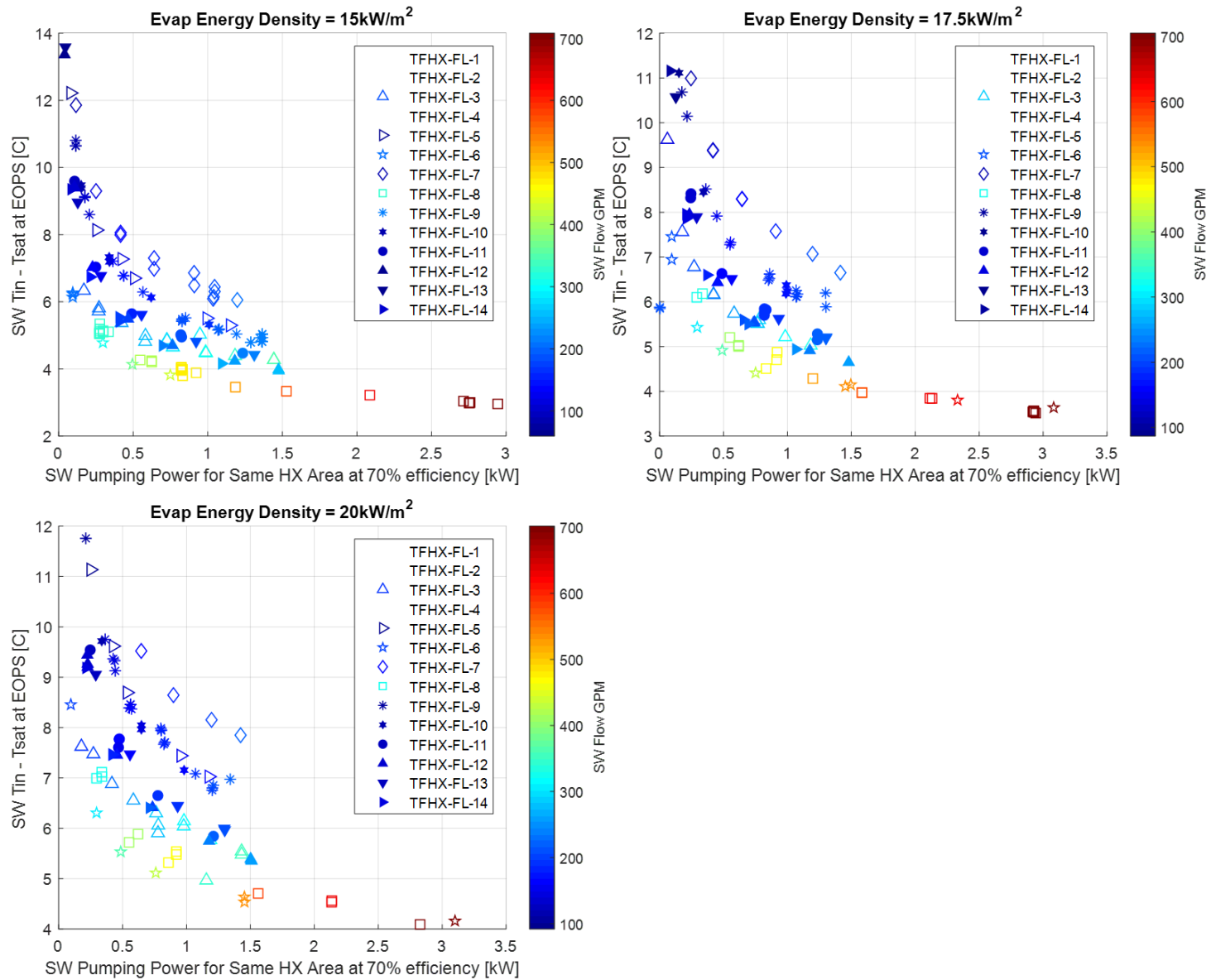
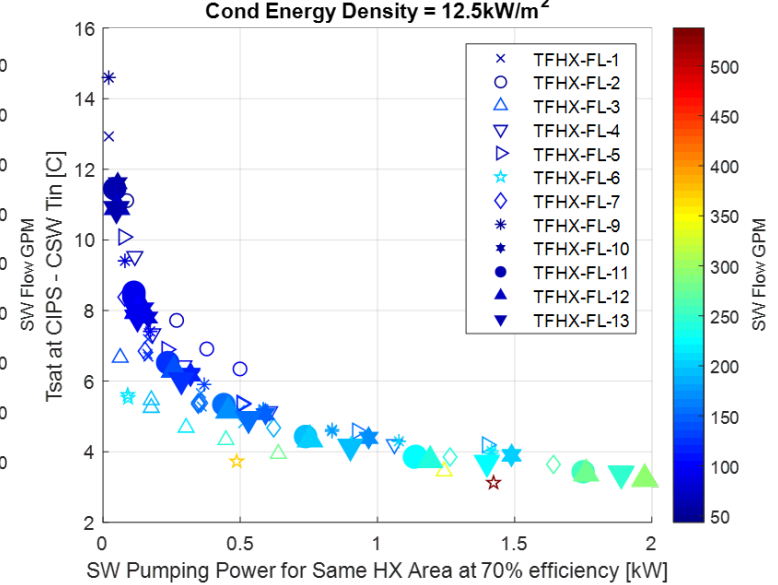
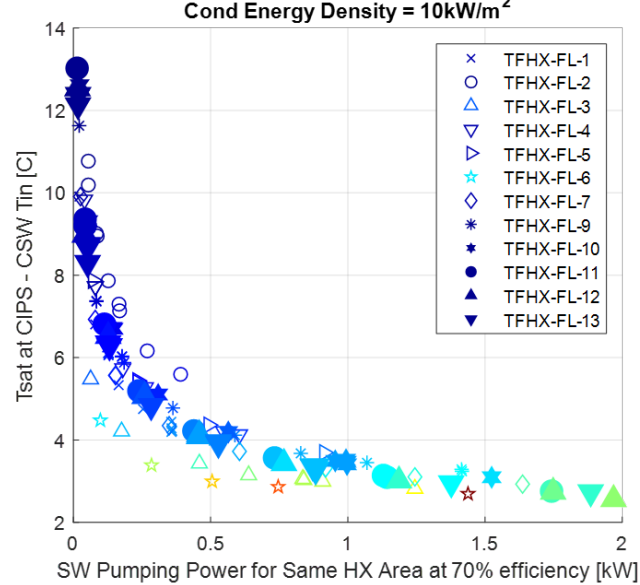
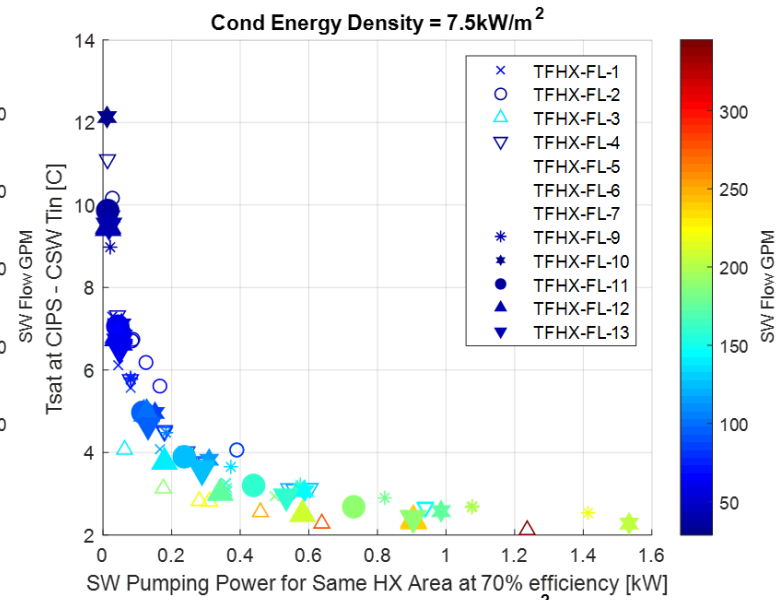
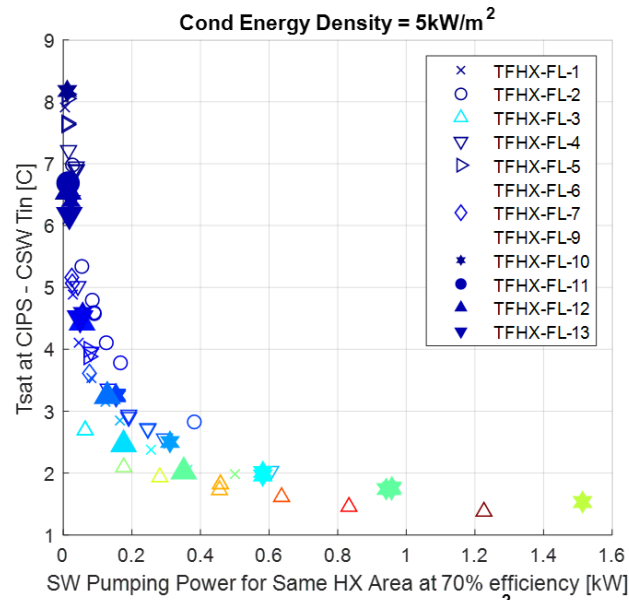


Figure 24. Evaporator approach temperature vs pumping power at different energy densities.



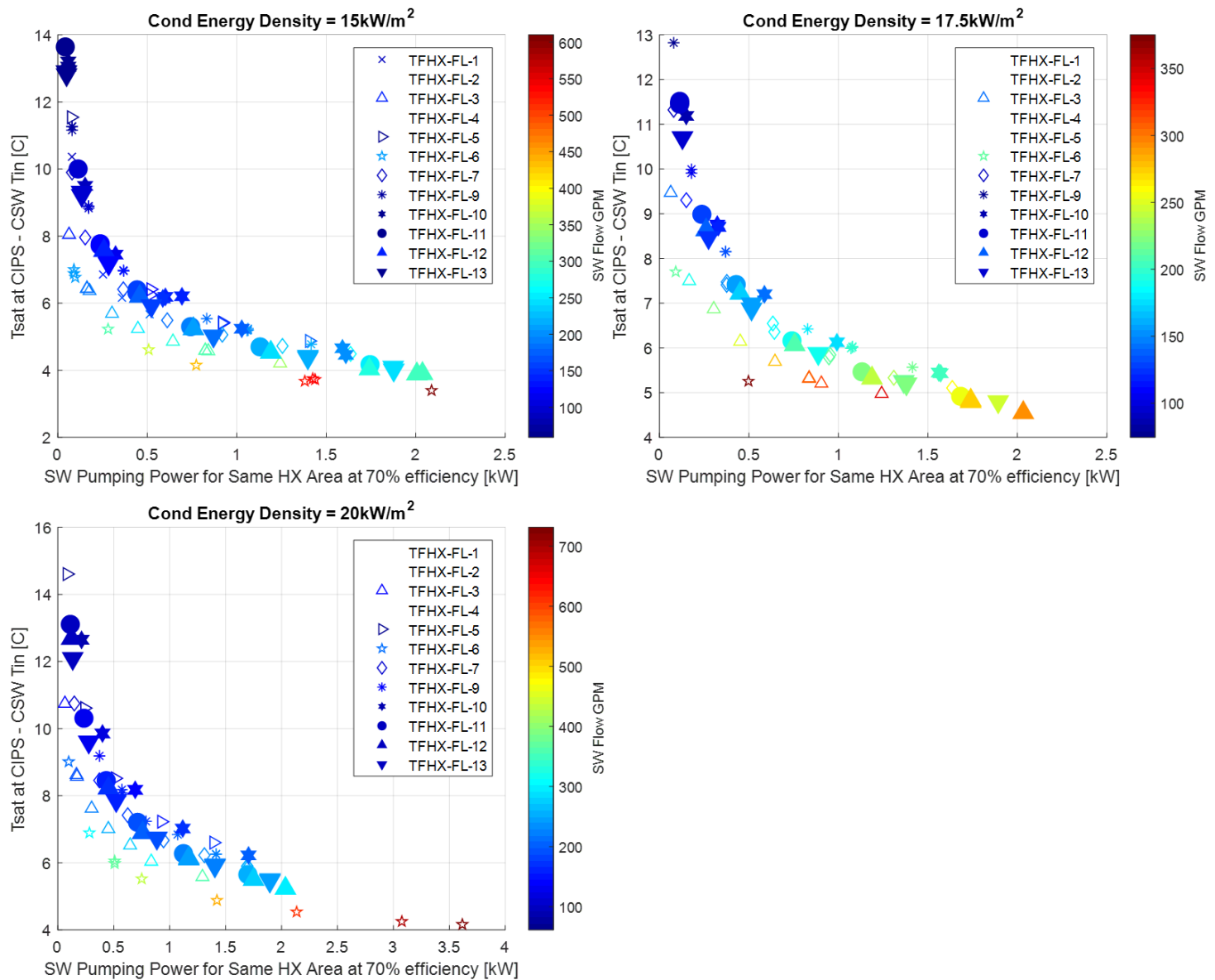
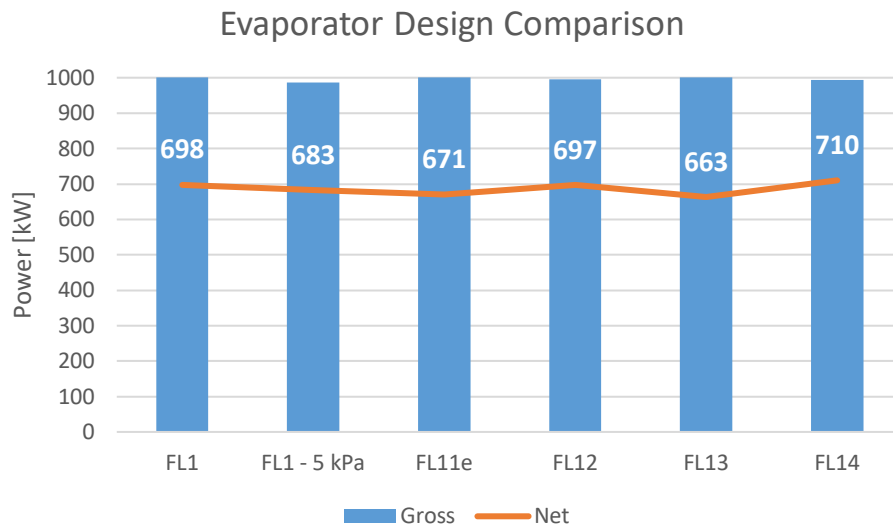


Figure 25. Condenser approach temperature vs pumping power at different energy densities.

#### 4.4. DISCUSSION

Makai previously reported on the development of the OTEC Power Calculator, a tool to evaluate different heat exchanger designs in the context of an OTEC system performance. Heat exchangers can be compared in terms of area (i.e., heat exchanger cost) or volume (i.e., system size and cost) required to produce a targeted net power. The calculator takes into account seawater flow rates through the heat exchangers *and* the system (cold water pipe, intake screen, discharge pipe).

The best heat exchanger design was established by setting the heat exchanger area and seawater temperature and varying seawater flow rates and turbine parameters to maximize net power. Previous results had FL-1 and FL-5 as the best performing evaporator and condenser, respectively. However, the optimal operating point was just outside the tested data range for FL-1, which led to some uncertainty in the results. FL-14 had the same design as FL-1 but internal channel size was slightly different. FL-14 was added to the previous OTEC Power Calculator analysis and produced 2% more net power compared to FL-12 for the same heat transfer area (Figure 26). However, the FL-12 design uses fewer welds compared to FL-14. A tradeoff between fabrication costs and performance led Makai to pick FL-12 to continue with large-scale seawater-ammonia testing.



*Figure 26. Comparison of evaporator designs in OTEC system.*

For condensers, FL-5 is still the overall best design (Figure 27). FL-13 is the next best design.

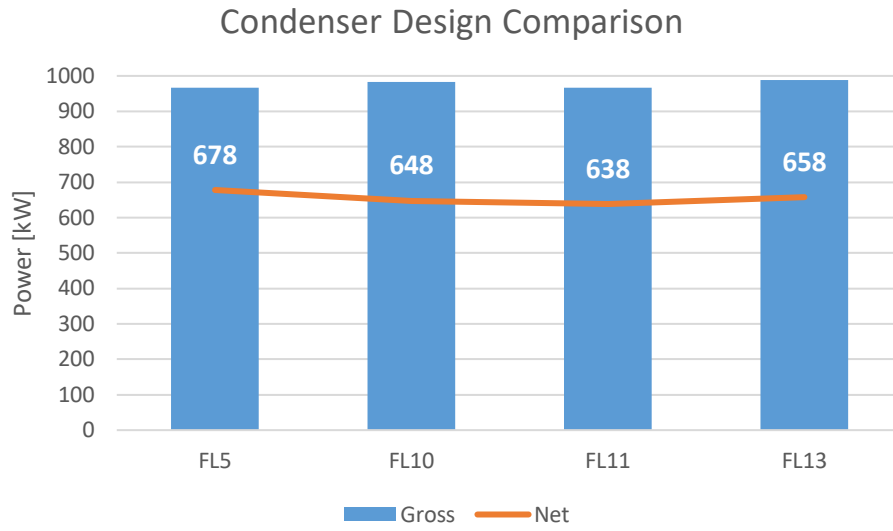


*Figure 27. Comparison of condenser designs in OTEC system.*

## 5. BIOFOULING

Untreated, biofouling can have a detrimental impact on heat exchanger performance by increasing the pressure drop through the heat exchanger and decreasing the heat transfer performance. Makai previously evaluated a commercially available biofouling mitigation device called the Zeta Rod and found it delayed the onset of biofouling by 30 days but eventually performance loss was comparable to the baseline (no mitigation) case. In this period, Makai continued testing a baseline and automated cleaning system.

### 5.1. INTAKE SCREEN TESTING

In addition to unfouled heat transfer surfaces, ensuring even flow distribution is a key factor in maintaining heat exchanger performance. The compact channels of the TFHX make it more susceptible to clogged seawater channels. At a 2.12-mm plate spacing, the effective seawater channel in the FL-12 design is only 1.22 mm. Even at the 3.5-mm plate spacing, the effective seawater channel is 2.6 mm. Over the past 10+ years of operating the HX Testing Facility at NELHA, Makai has observed much larger objects (shells, rocks, even shrimp) in seawater supply. These are currently filtered through a strainer which requires periodic cleaning to remove accumulated particles at the bottom of the strainer and fibrous mats on the sides of the strainer (Figure 28).



*Figure 28. Strainer inspection revealed accumulated shells at the bottom and fibrous mats on the sides.*

A screen is necessary to prevent debris from blocking the flow channels in the TFHX; however, the screen itself is a surface that can become clogged from biofouling. Makai is testing a screen to evaluate how it performs when immersed in tropical surface seawater and exposed to different types of biofouling. The intake screen test is in the same tank as the submerged biofouling test. During the diatom bloom, the uncleaned surfaces appeared fouled whereas the screen itself remained clean.

## 6. SUMMARY

Between February 2024 – October 2024, Makai improved TFHX plate fabrication speed and success rate; constructed and performance tested additional full-length TFHX units; constructed and assembled two cassette-style 2-MW<sub>thermal</sub> TFHXs; developed concepts for large-scale seawater-water TFHXs; and prototyped new biofouling mitigation methods.

*TFHX Design and Characterization.* Makai installed a pass-thru seawater air conditioning (TFAC) in the corrosion lab to replace a failed AC fan unit. The TFAC has been operational for over 2 months and is functioning as expected. Makai previously delivered a TFAC unit to Blue Ocean Mariculture as a case study but it was never placed in service.

Makai also constructed and installed two 300-plate seawater-ammonia TFHXs. One 2-MW<sub>thermal</sub> condenser and one 2-MW<sub>thermal</sub> evaporator have been installed on the new HX Testing Tower and Makai expects to commission and begin testing in the next period. These heat exchangers will provide bounds on the accuracy of using 100-kW test data to predict the performance of large-scale heat exchangers required for OTEC systems.

For large-scale seawater-seawater/water applications, Makai has developed new housing concepts that incorporate the cassette-style installation for the plate stack and in-situ biofouling cleaning. Makai intends to construct a prototype-scale unit and conduct initial performance testing at NELHA. Makai is holding discussions with HECO to test this prototype unit as a long-term case study at the Kahe Point power plant. In order to meet the performance and pressure drop requirements for seawater-seawater/water applications, Makai has been designing plates with larger internal channels and testing variations of increased insert size to meet the larger plate spacings required when using larger internal channels.

*TFHX Fabrication.* Makai improved the overall plate success rate to ~90% from ~60% by improving subsystems, operation processes, better defect identification algorithms and implementing post-expansion repair. Most importantly, Makai has been able to demonstrate *consistency* in success rates over multi-day fabrication runs with a skilled operator. Makai is now developing methods and fixtures to automate portions of the process to reduce time and remove operator skill from the fabrication process.

*TFHX Performance Testing.* In this period, Makai tested one ammonia-seawater (OTEC) four-port TFHX and two seawater-seawater four-port TFHXs. Ammonia-seawater performance data is fed into the OTEC Power Calculator to evaluate the different TFHX designs in the context of an OTEC power plant. The OTEC Power Calculator accounts for parasitic losses related to the total amount of seawater flow through the system, not just through the heat exchangers.

TFHX designs tested in this period were compared to previous designs in the OTEC Power Calculator. The best designs were TFHX-FL14 and TFHX-FL4 for the evaporator and condenser, respectively. However, Makai selected TFHX-FL12 as the new evaporator design because it has 2/3s as many welds as FL14 (i.e., easier to fabricate) and is predicted to produce only 2% less net power compared to TFHX-FL14.

*Biofouling.* Makai continued the automated and baseline biofouling tests. Both tests have been operating for ~10 months. In the baseline test, the pressure drop has increased 347% since the Day 0 measurement whereas in the automated cleaning test, pressure drop has only increased 10% over Day 0 measurement.

#### *Upcoming Work*

The major points of focus for Makai's near-term work are to:

- Performance test the 2-MW<sub>thermal</sub> TFHXs to ground truth performance predictions based on 100-kW scale test data
- Continue to develop cost-effective designs for large-scale seawater-seawater/water applications
- Improve the speed and variability in TFHX plate fabrication time and success rate through automation to remove dependence on operator skill
- Continue to develop, prototype and test in-situ biofouling control/mitigation systems